

ADDIS ABABA UNIVERSITY

ADDIS ABABA INSTITUTE OF TECHNOLOGY

SCHOOL OF CIVIL AND ENVIRONMENTAL ENGINEERING



Fracture Mechanics in Concrete and its Application on Crack Propagation and Section Capacity calculation

A Thesis in Structural Engineering

By Andargachew Mekonen

18/02/2018

Addis Ababa

Submitted in Partial Fulfillment of the Requirements for the Degree
of Master of Science

ADDIS ABABA UNIVERSITY-ADDIS ABABA INSTITUTE OF TECHNOLOGY
SCHOOL OF CIVIL AND ENVIRONMENTAL ENGINEERING

“Fracture Mechanics in Concrete and its Application on Crack Propagation and Section Capacity calculation”

By

Andargachew Mekonen

Approved by the Board of Examiners:

Asnake Adamu (PhD)

Advisor

Signature

Date

Adil Zekaria (PhD)

Internal Examiner

Signature

Date

Esayas G/Youhannes(PhD)

External Examiner

Signature

Date

.....

Chairman

Signature

Date

Acknowledgement

First of all, I would like to thank to my MSc advisor, Dr. Asnake Adamu, for supporting me during my thesis work and sharing his great knowledge and experience with me. Without his supervision and constant help, this Thesis would not have been possible. Under his guidance I successfully overcame many difficulties and learned a lot. It has been an honor to be his student.

I will forever be thankful to Mr. Bayelign, Solomon, Garomisa and Tina for their helping and Advise to complete the final goal of my thesis, Especial thanks for Liyuye, you were my strength when I was doing my thesis.

I would like to pay high regards to my Family who I love for their sincere encouragement and inspiration thorough my research work and lifting me uphill this phase of life. I owe everything to them.

Last but certainly not least, I would like to thank my family members and friends for their invaluable support.

Contents

List of Tables	v
List of Figures	vi
List of symbols.....	viii
Abstract	x
1 Introduction.....	1
1.1 Background.....	1
1.2 Objective and Scope of the study.....	1
1.3 Thesis organization	2
2 Literature Review on Fracture Mechanics.....	3
2.1 Introduction.....	3
2.2 Types of Fracture and Basics of Fracture Mechanics	5
2.2.1 Types of Fracture	5
2.2.2 Fracture Energy.....	6
2.2.3 Stress Intensity Factor (SIF) (KI)	9
2.2.4 An Atomistic View of Fracture.....	10
2.2.5 Types of Fracture Mechanics.....	13
i. Linear Elastic Fracture Mechanics	13
ii. Nonlinear Fracture Mechanics (Elastic-Plastic FM)	19
2.3 Cracks in Reinforced Concrete Structures	22
2.3.1 Variation of Tensile Strength of Concrete	23
2.3.2 Code Provision of Cracks	23
2.4 Section Capacity of Reinforced Concrete Elements.....	40
2.4.1 Stress and strain diagram	40
2.4.2 Code provisions on stress strain diagram.....	43

3 Fracture Mechanics of Concrete	48
3.1 Pre/Post-Peak Material Response of Steel and Concrete.....	48
3.2 Stress versus crack opening displacement Diagram	49
3.3 Concrete Models for Fracture Analysis	50
3.3.1 Fictitious crack model (Cohesive Crack Model)	50
3.3.2 Crack Band Model (CBM).....	51
4 Application of Fracture Mechanics.....	54
4.1 Numerical Approach of Fracture Mechanics	54
4.2 SIF and propagation criteria.....	55
4.3 Proposed crack propagation model	58
4.4 Proposed section capacity model	71
4.5 Fracture Mechanics using Finite element software	74
4.6 Numerical Examples	76
4.7 Comparisons and Discussions.....	91
5 Conclusion and Recommendations.....	95
5.1 Conclusions.....	95
5.2 Recommendations.....	96
References.....	97
Appendix.....	100

List of Tables

Table 2. 1: Applicability of EPFM and LEFM.....	22
Table 4. 1: Geometric parameters of the test specimens	76
Table 4. 2 : Reinforcement Design Data.....	76
Table 4. 3: EBCS 2, 1995 Critical Load	78
Table 4. 4: ACI critical Load	79
Table 4. 5: EC 2, 2004 Critical Load	79
Table 4. 6: Proposed Model Critical Load.....	82
Table 4. 7: ACI moment capacity	83
Table 4. 8: EU 2, 2004 Moment capacity	84
Table 4. 9: EBCS 2, 1995 Moment capacity	84
Table 4. 10: Proposed Model moment capacity.....	85
Table 4. 11: initial crack length, width and length of the specimens.....	89
Table 4. 12: Stress intensity factors and energy release rate for plane stress and plane strain conditions.....	90
Table 4. 13: Cracking for different building codes under different cross section	91
Table 4. 14: Moment capacity of a cross section under different building design codes and Propose model.....	92

List of Figures

Figure 2. 1: Three basic modes for cracked body :(a) Mode I (b) Mode II (c) Mode III, [18].....	5
Figure 2.2 : Plate with crack length a, [2].....	6
Figure 2.3 : Plate with elliptic hole subjected to tension, [5].	7
Figure 2.4: Amount of Energy and corresponding crack length,.....	8
Figure 2. 5: Elastic stress distribution near crack tip, [5]	10
Figure 2.6: The energy curve (top) and force versus dislocation radius, [4]	11
Figure 2. 7: crack tip variables for Sharp crack, [6]	14
Figure 2. 8: Response of three point bend specimens with initial crack length a_0	15
Figure 2. 9 : Crack tip stress conditions, [7]	16
Figure 2. 10 : Crack tip radius for elastic and plastic zone, [4]	17
Figure 2. 11: Stress conditions causing opening and closing of crack tip, [2]	17
Figure 2. 12 : The fracture Process Zone developed beyond the crack is large enough to be considered, [6].....	19
Figure 2.13: Blunted crack beyond the sharp crack, [5]	20
Figure 2. 14: Shows crack tip opening displacement [5].....	20
Figure 2. 15: Quarter points and collapsed elements, [5]	32
Figure 2. 16: a) Plate corner with included angle; b) Special case of sharp Crack, [5].....	33
Figure 2. 17: Orientation of the crack plane, [5].....	33
Figure 2. 18: Biaxial loading for Westergaard solution, [14].....	36
Figure 2. 19: Plate subjected to far field stress, [2]	38
Figure 2. 20: Section body, [14]	40
Figure 2. 21: Tractions decomposition, [14].....	41
Figure 2. 22: EBCS 2, 1995 provision for stress-strain diagram for concrete under compression, [18].....	43
Figure 2. 23: EU 2, 1994, provision for Parabolic-rectangular stress-strain diagram for concrete under compression, [17].....	44
Figure 2. 24: EU 2, 1994, provision for bilinear stress-strain diagram for concrete under compression, [17].....	44
Figure 2. 25: Typical Concrete stress-strain curve according to ACI provision, [10].....	45

Figure 2. 26: Typical concrete stress-strain diagram under compression with different compressive strength, [10]	45
Figure 2. 27: Stress-strain and stress-displacement diagram for concrete section, [10].....	46
Figure 2. 28: Dependency of the stress-strain diagram in the depth of compression zone, c, [10]	47
Figure 3. 1: Stress-Strain Curves of reinforcement bars and Concrete, [28].....	48
Figure 3. 2: Hillerborg Fictitious Crack Model, [28].....	51
Figure 4. 1: Plate subjected to far field tensile stress with central hole,.....	60
Figure 4. 2: The plane stress and plane strain plastic zone, [5]	61
Figure 4. 3: Area of special curve called Lemniscate,.....	61
Figure 4. 4: Approximate process zone beyond crack tip.....	61
Figure 4. 5: Transverse and longitudinal section of three point bend beam	63
Figure 4. 6: Beam subjected to central loading.....	68
Figure 4. 7 : Beam part near the crack	68
Figure 4. 8: Magnified view in the vicinity of the crack	68
Figure 4. 9: Stress carried by rebars and concrete, [29].....	69
Figure 4. 10: Simple linear softening Model, [28].....	70
Figure 4. 11: Linear strain distribution for flexure type loading	72
Figure 4. 12: Beam subjected to two point Loading	76
Figure 4. 13: Stress-strain diagram for reinforcement	76
Figure 4. 14: Cracking loads versus size using different building codes and Proposed model	91
Figure 4. 15: Section capacity varies with beam size using different building codes and Proposed Model	92
Figure 4. 16: a) Variations of stress intensity for mode I with proportion crack growth	94

List of symbols

a	= initial crack length
a_{cr}	= critical crack length
A	= area of concrete
A_s	= area of tensile longitudinal steel reinforcement
[B]	= element strain-displacement matrix
CMOD	= crack mouth opening displacement
c	= Plastic zone length
C	= Depth of compression zone
d_a	= maximum aggregate size
d	= Distance from the extreme compression fiber to the centroid of the Longitudinal tension reinforcement
[D]	= material stiffness matrix
E	= Young Modulus
E_b	= Bond energy between atoms
f_c	= concrete cylinder uniaxial compressive strength
f_{ct}	= specified mean tensile strength
f_r	= modulus of rupture strength
G	= Energy release rate
J	= nonlinear energy release rate
k	= Bond stiffness
K_I	= Mode I stress intensity Factor
K_{II}	= Mode II stress intensity Factor
K_{III}	= Mode III stress intensity Factor

M_u	= ultimate moment
R	= crack resistance force
r_y	= plastic zone using elastic analysis
r_p	= plastic zone using plastic analysis
U_a	= Surface energy
U_d	= dissipated Energy
U_e	= total input energy to the system
U_i	= internal strain energy
U	= kinetic energy
w	= average crack width
W	= Energy density function
Z	= empirical value to control cracks
β	= Brittleness number
ε_{ch}	= characteristic strain for concrete in tension
ε_{cr}	= concrete cracking strain
ε_{cx}	= average net concrete axial strain, in the x-direction
ε_{cy}	= average net concrete axial strain, in the y-direction
ε_{sm}	= mean strain of the reinforcement
θ	= angle of crack inclination
ρ_x	= longitudinal tensile steel reinforcement ratio
ρ_y	= transverse steel reinforcement ratio
σ_x	= applied axial stress in the x-direction
σ_y	= applied axial stress in the y-direction
τ_{xy}	= applied shear stress

Abstract

Reinforced Concrete structures have been designed for long time using the Elastic and Plastic limit state theories. However, real life experiences shows that these theories are not sufficient for having the expected Failure Mode which is called Ductile Failure. In the Limit States theory, one of the major drawback is, it assumes strength as a material property independent of size. But in reality, the size effect is significant phenomena in controlling the failure mode. Limit States theory missed the concept of Size Effect. The basic concept behind the Size Effect is, as the size of the material increase, the volume of micro cracks and flaws also increase. This internal micro cracks and flaws are points where stress concentrations occurs. Through time, these micro crack and flaws will develop in to macro cracks. Therefore, the strength (Tensile and compressive) are dependent on Material member length and cross section.

In this Thesis, crack propagation and section capacity for Reinforced Concrete structures are analyzed using the size effect concept which is addressed using Fracture Mechanics

1 Introduction

1.1 Background

In order to properly determine the real response of a structure, it is reasonable to use parameters which are totally independent of structure size. Till this days almost all building codes for reinforced concrete structures use the limit state theory, basically the elastic and plastic limit analysis. However in both limit states, the response of the structures are expressed interms of parameters which are dependent of size. One of the most common parameters to be used for in analysis and design is tensile strength of concrete. Experiences shows that there is a possibility of a given reinforced concrete elements to fail before the load reaches to its peak value. As long as the real structures are not tested in laboratory, it is quite easy to sense that there will be variations between the predicted and actual response. When this variation is significant it is rational either to change the parameters (tensile strength and compressive strength) which are used to express the response of the structures or apply some modifications for limit state analysis output.

Therefore, to properly capture the real response of reinforced concrete elements, the response should be expressed Intermis of size independent parameters. Real life experience like those of diagonal shear failure of beam, punching shear failure of slabs and pull out failures of reinforcement bars are clear indications for the existence of size effect. The worst case scenario which can happen at any time is, the failure mode caused by ignorance of size effect is brittle. This failure can happen at any time without any prior sign. As much as possible it is advisable to consider all the possible sources of brittle failure mode.

1.2 Objective and Scope of the study

The main objective of this research is to introduce and apply the Basic Fracture Mechanics concepts for reinforced concrete structures for crack related issues and section capacity calculations issues related with stress strain diagram.

Basic Fracture Mechanics concepts with some modifications will be used effectively for better predictions of reinforced concrete elements response for Mode I (Flexural type) cracking type. Special focus will be given to implementation of Fracture concepts for reinforced concrete structures.

1.3 Thesis organization

The Thesis is organized into five chapters. Chapter 1 deals with the general introduction and the need for further study in the field of crack propagation and section capacity for reinforced concrete structures.

Chapter 2 covers literature reviews on fracture mechanics. As this science was used mainly for metals, general introductions are discussed using simple concepts. In addition, code prescriptions for crack propagation and section capacity are also elaborated. A critical concept of stress and strain in the vicinity of the crack tip has been also discussed with special finite elements.

Chapter 3 provides information on the pre and post peak nature of reinforced concrete structures. The need for having a stress-crack tip opening displacement diagram is also discussed. Ideas on recent advances on concrete modeling for fracture analysis are also provided.

Chapter 4 states about the application of fracture mechanics for reinforced concrete structures. Basic fracture parameters like stress intensity factors are also discussed. Assumptions for the two proposed models with numerical examples are also included in this chapter. Comparisons of code-based formulas and proposed model results are also given in this chapter. Conclusion and recommendations are discussed in chapter 5.

2 Literature Review on Fracture Mechanics.

2.1 Introduction

When Reinforced concrete structures are subjected to general loading conditions, failure is inevitable. Failure can be caused by uncertainties in loading, defects in materials, inadequate design, and deficiencies in construction and maintenance and for some other reasons. In the process of failure, structure changes its original shape and deformation is exhibited. In the deformation process bodies of the material get separated and the load bearing capacity of the structures abruptly decrease and it may approach to zero. This deformation process whereby regions of body get separated is called Fracture. Fracture is defined when the applied loading of a cracked body (crack driving force) exceeds the Material's resistance to failure (fracture toughness).

Fracture Mechanics deals with mechanics of solids containing displacement discontinuities (cracks) with special attention for crack growth. It is also defined as failure theory that determine material failurity, possibly in conjunction with the strength (yield) criteria. In the plastic limit analysis, failure is assumed to be simultaneous throughout the structures. However in the real case failure is more propagating and redistribute in every direction rather than simultaneous and one way.

Till this days almost in all building codes, concrete structures are designed and successfully built using the concrete building codes which totally ignores the Fracture Mechanics. However, this does not mean that the codes are okay but two simple understanding can be developed. One is the load factors and material capacity reduction factors can possibly hide the effect. For instances the deal load factor is 1.4, this means 40% of additional loads are assumed and for live load, 60% of additional live loads are included. This assumptions are totally irrational but since the real failure mechanisms are not known clearly, there is no other option than to use high load factors for safe and uneconomic design.

Real life experiences shows that it is rational to consider the size effect. One way of considering size effect is to use the basic concepts of Fracture Mechanics. There are different compelling reasons for using Fracture Mechanics concepts for concrete structures. In the process of deformations cracks will be created. The formation of this crack can be related with surface energy which is used for creation of new surface, [1].

When crack occurs, new surface is created at the same time. This shows that crack formation is related with energy one way or the other way. In Fracture Mechanics, Energy related with crack formation has got great attentions. Besides the current strength based analysis and design results show that some important material parameters are independent of size. In the limit analysis, strength is expressed as material property which is independent of size. However experiments shows that materials like reinforced concrete structures shows load deflection which is neither similar to ductile materials nor like those of brittle material. From the load deflection diagram, it is concluded that reinforced concrete structures are quasi brittle material. Therefore, better prediction of response can be obtained if Fracture Mechanics with some modification is used.

In addition, it is rational at least to minimize the rate of occurrence of brittle mode of failure. One way of making sure that the failure mode is ductile is to consider the amount of energy absorbed and ductility nature of the material. The simplest principle is to make sure that the strain energy of the given cross section is less than the amount of energy required for creation new surface. In the Fracture Mechanics one of the most known size independent parameter is Fracture Energy. Fracture Energy is defined as the specific energy required for crack growth in an infinite large specimens. The main importance of this definition is to eliminate the effect of sizes, shapes and type of loading on the fracture energy. This basic parameter needed for rational predictions of brittle failure of concrete structures. Another very important parameter is the Fracture Process Zone (FPZ). This is a zone where softening occurs. It is a place where Fracture initiates, [2].

Finally, it is observed that plastic limit analyses provide no information on the post peak load deflection diagram and the amount of energy dissipated in the fracture process. However, using Fracture Mechanics, information lost in plastic limit analysis can be captured, [2].

2.2 Types of Fracture and Basics of Fracture Mechanics

2.2.1 Types of Fracture

Once the crack is nucleated on the surface of the structure, its growth occurs in presence of a very high gradient associated stress field. Three basic modes for crack growth are defined in many literatures. These are Mode I, which is the “opening” or “tensile mode”, where the crack faces separate symmetrically with respect to the x_1-x_2 and x_1-x_3 planes. In Mode II, the “sliding” or in “plane shearing” mode, the crack faces slide each other symmetrically about the x_1-x_2 plane but anti-symmetrically with respect to the x_1-x_3 plane. In the “tearing” or “anti-plane” mode, Mode III, the crack faces also slide each other but anti symmetrically with respect to the x_1-x_2 and x_1-x_3 planes. In several practical cases, loads excite simultaneously two modes and make the crack propagation depending on a so-called “mixed-mode fracture mechanism” [4]. In this paper only Mode I type of crack is given attention, [18].

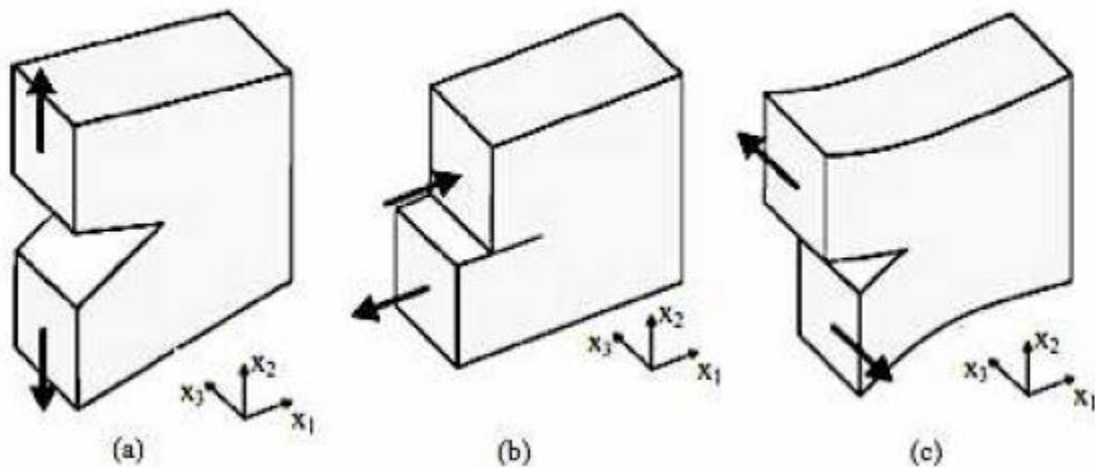


Figure 2. 1: Three basic modes for cracked body :(a) Mode I (b) Mode II (c) Mode III, [18].

2.2.2 Fracture Energy

For a system of constant temperatures, first law of thermodynamics states that the total amount of energy that is supplied to a material volume per unit of time (\dot{u}_e) must be transferred to the internal energy(\dot{u}_i) surface energy(\dot{u}_a) dissipated energy(\dot{u}_d) and kinetic energy(\dot{u}_k).

The internal energy is the elastically stored energy, the surface energy comes in to effect when crack propagates, the kinetic energy is function of material speed and finally the dissipated energy is due to friction and plastic deformation.

In Fracture process, the surface of the crack varies so it can be taken as state variable. If the thickness, b , is assumed to be constant, the only state variable will be the crack length, a . Since Area= $b \cdot a$.

When crack happens in material, the internally stored energy acts as source of energy. For the figure below assume the width, b , to be constant,

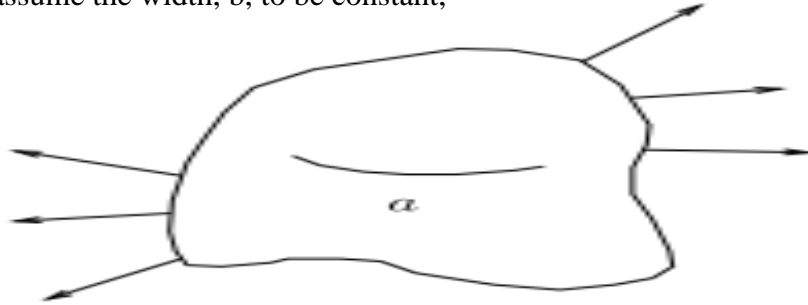


Figure 2.2 : Plate with crack length a , [2].

Using first law of thermodynamics

$$\dot{U}_e = \dot{U}_i + \dot{U}_a + \dot{U}_d + \dot{U}_k \quad [JS^{-1}] \quad (2.1)$$

From simple calculus using Change of Variables

$$\frac{du_e}{dt} = \frac{dA}{dt} \frac{du_e}{dA} = b \frac{da}{dt} \frac{du_e}{bda} = a \frac{du_e}{da}$$

If the dissipated energy and kinetic energy are neglected, the available external energy and internal energy is transferred to surface energy.

$$\frac{du_e}{da} = \frac{du_i}{da} = \frac{du_a}{da}$$

This equation is called Griffith energy balance.

Divide both side by b yields the Energy Release Rate (G)

$$G = \frac{1}{b} \left[\frac{du_e}{da} - \frac{du_s}{da} \right]$$

And the Crack Resistance Force (R)

$$R = \frac{1}{b} \left[\frac{du_a}{da} \right]$$

Griffith crack criteria $G = R$

For the case of fixed grips ($u = 0$)

$$\frac{du_e}{da} = 0 \rightarrow -\frac{du_i}{da} = \frac{du_a}{da}$$

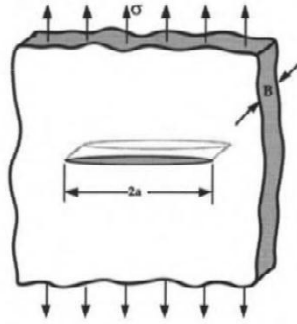


Figure 2.3 : Plate with elliptic hole subjected to tension, [5].

The total surface energy for the above in through elliptical crack, where γ_s is surface energy and K is some constant, can be calculated as shown below

$$u_a = K * a = 4ab\gamma_s$$

The total strain energy (internal energy)

$$u_i = 2\pi a^2 b \frac{\sigma^2}{2E}$$

Using Griffith criteria, for crack to propagates $G = R$

$$2\pi ab \frac{\sigma^2}{2E} = 4b\gamma$$

From the above the critical crack length will be

$$a_{cr} = \frac{2\gamma_s \dot{E}}{\pi\sigma^2} \quad (2.2)$$

Where \dot{E}

$$\dot{E} = \begin{cases} E & \text{for plane stress} \\ \frac{E}{1-\nu} & \text{for plane strain} \end{cases}$$

Energy available (source of energy) $U_i = -2\pi a^2 b \frac{\sigma^2}{2E}$

Energy needed for new surface generation $U_a = 4a b \gamma_s$

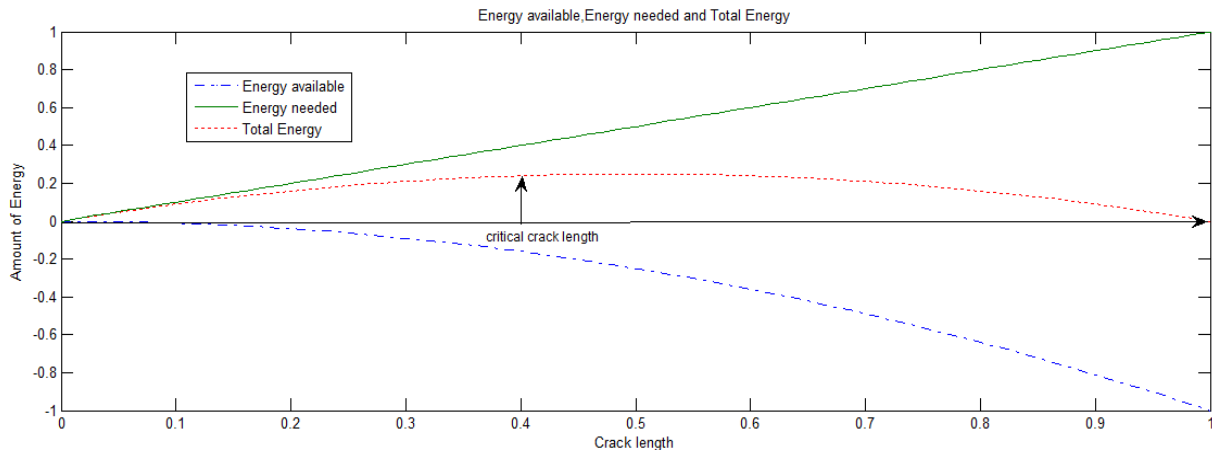


Figure 2.4: Amount of Energy and corresponding crack length,

In Griffith energy balance, energy dissipated in the system is neglected. This causes a discrepancy between the experiment and analytic values. The discrepancy between the experiment and analytically calculated values can be shown by both the stress and energy approach.

For materials which are very brittle, the amount of energy dissipated is very small, enough to be ignored when crack growth. But for ductile materials, showing significant energy dissipation the energy release rate can be 10^5 times the crack growth resistance force (R), [15].

For brittle material

$$\sigma_c = \sqrt{\frac{2\gamma_s \dot{E}}{\pi a}}$$

And For Ductile material

$$\sigma_c = \sqrt{\frac{2(\gamma_s + \gamma_p) \dot{E}}{\pi a}}$$

Where γ_s plastic work per unit area of surface created. For ductile material $\gamma_s \gg \gamma_p$, this shows ignoring or neglecting the amount of energy dissipated can be a source of erroneous result. Energy release rate (G) can be calculated using different techniques like those of fixed and constant loads. In both techniques for energy release rate (G) determination, compliance, which is the ratio of opening to force, approach will be used. G can also be calculated from the force displacement curve, [4].

2.2.3 Stress Intensity Factor (SIF) (K_I)

Stress Intensity Factor (SIF) (K_I) is a measure of stress intensity in the vicinity of the crack tip. Higher SIF means larger stress pattern at the tip of the line crack continuum. It is measured in $\text{MPa}\sqrt{m}$. The subscript I shows that the SIF is for the mode I or open type cracking.

If the stress is applied perpendicular to crack width with sharp tip, the linear elastic solution shows that stress concentration will appear at the tip such that the stress approaches to infinity. Close to the crack tip the stress distribution is approximated by

$$\sigma_y = \frac{K_I}{\sqrt{2\pi x}} \tag{2.3}$$

Where, x is the distance from crack tip and K_I is Stress Intensity Factor, (SIF).

This factor can be calculated from $K_I = Y\sigma\sqrt{a}$

Where a is crack width, σ stress where crack length is zero and Y is dimensionless factor often taken as 2.

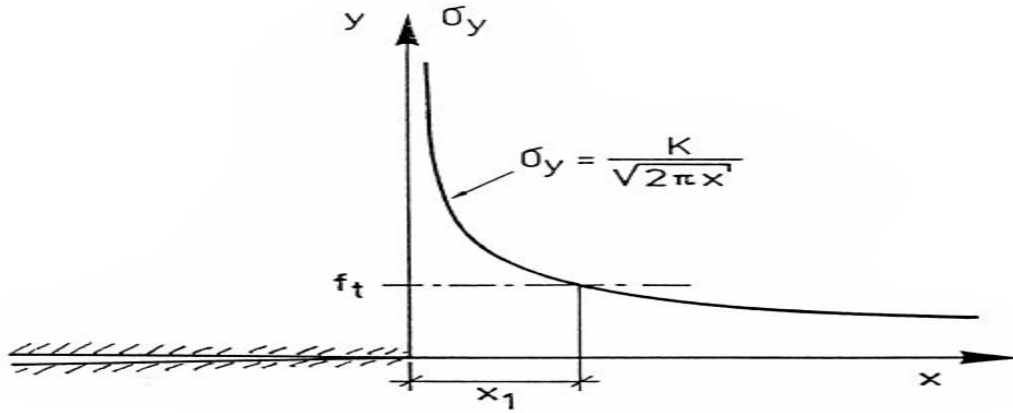


Figure 2. 5: Elastic stress distribution near crack tip, [5]

As the stress approaches infinity, the analysis of crack stability and crack propagation cannot be based on the comparison with the strength of material. At this point it is rational to introduce new criterion which dictates that crack will start propagating when the SIF reaches a critical values, K_{Ic} , which is assumed to be material property, [5].

SIF is used in analysis and design by arguing that material can with stand crack tip stress up to a critical value of stress intensity termed as K_{Ic} beyond which the crack propagate faster. This K_{Ic} measures material toughness.

Failure stress then calculated to the crack length a and fracture toughness K_{Ic} by

$$\sigma_f = \frac{K_{Ic}}{\alpha\sqrt{\pi a}} \quad (2.4)$$

Where $\alpha = 1$ for edge crack and different α can be found for different crack positions. Generally SIF can be expressed as $K_I = \beta\sigma\sqrt{\pi a}$ where β depends on the location of pre-existing notch, [24].

2.2.4 An Atomistic View of Fracture

The bond strength that exist between atoms plays a great role when the issues of Fracture arises. This is mainly because failure occurs when only the stress developed between atoms is greater than the bond stress that already exist. The stress developed is supplied by the external load while the force of attraction between atoms is the main source of the bond stress.

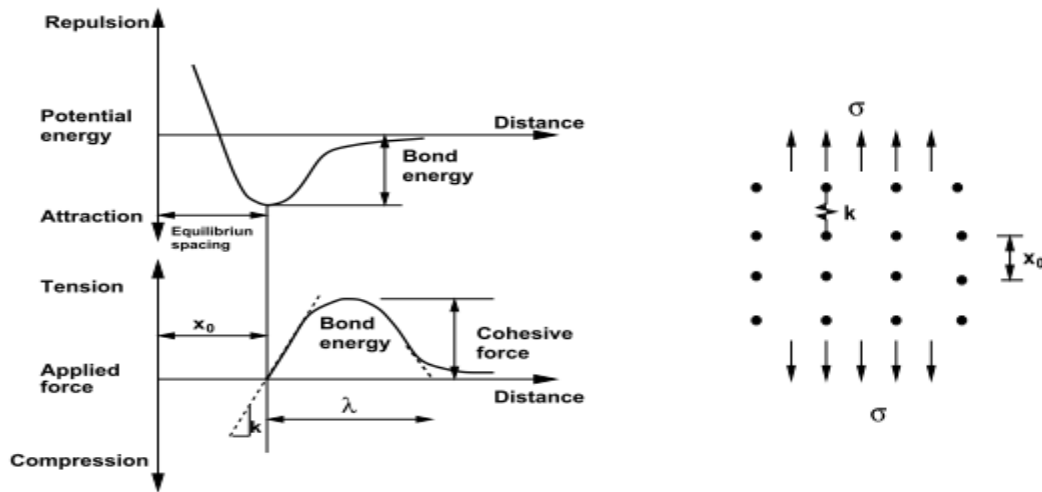


Figure 2.6: The energy curve (top) and force versus displacement, [4]

From the figure at $x = 0$, the force between atoms is null. This distance is called equilibrium spacing.

The area under the force versus displacement of atoms gives the amount of energy needed to displace the atoms and cause failures, and it is called Bond energy (E_b)

$$E_b = \int_{x_0}^x P dx$$

Where, P is the applied force. By assuming of one half the period of sine wave for the interatomic force displacement relationships

$$P = P_c \sin\left(\frac{\pi x - x_0}{\lambda}\right)$$

With the origin defined at X_0 .

For very small displacement $\sin x \approx x$, using the same analogy

$$P = P_c \left(\frac{\pi x - x_0}{\lambda}\right)$$

The above equations can be simplified as

$$F = K\Delta x$$

Where $\Delta x = x - x_0$, $K = P_c \left(\frac{\pi}{\lambda} \right)$ and $F = P$

Therefore, the bond stiffness is

$$K = P_c \left(\frac{\pi}{\lambda} \right)$$

$$K * \lambda = P_c * \pi$$

Since $K = \frac{P}{\Delta x}$

$$\frac{P}{\Delta x} \lambda = P_c * \pi \quad \text{for } P = P_c$$

$\lambda = \Delta x * \pi$, Dividing both side by x_0

$\frac{\lambda}{x_0} = \varepsilon * \pi$ Since $\varepsilon = \frac{\sigma}{E}$ and rearranging Where E is elastic Modulus and σ_c is cohesive strength.

Finally the cohesive strength can be expressed in simple form as:

$$\sigma_c = \frac{E * \lambda}{\pi * x_0}$$

For $x_0 = \lambda$, the theoretical cohesive strength can be simplified to the form

$$\sigma_c = \frac{E * \lambda}{\pi * x_0} \tag{2.5}$$

It is clear that there will be some energy requirements for the new surface to be created. Let the energy required to create single surface is surface energy denoted by γ_s

$$2^* \gamma_s = \int_{x_0}^{\lambda+x_0} \sigma \, dx$$

$$\gamma_s = \frac{1}{2} \int_0^\lambda \sigma_c \sin\left(\frac{\pi x}{\lambda}\right) dx = \sigma_c \frac{\lambda}{\pi}$$

This shows that the Fracture energy is about two times of the surface energy.

Finally after some simplifications

$$\sigma_c = \sqrt{\frac{E^* \gamma_s}{x_0}} \quad (2.6)$$

The theoretical cohesive strength is approximated to be $\frac{E}{\pi}$. However, due to the presence of flaws there will be discrepancy between the theoretically calculated and experimentally obtained values. But the basic point here is Fracture can never occur unless the defects play a role in magnifying the stress around so that the magnified stress will be greater than the normal cohesive strength, [6].

2.2.5 Types of Fracture Mechanics

Based on the size of the Fracture Process Zone (FPZ), there are two types of Fracture Mechanics. These are Linear Elastic Fracture Mechanics (LEFM) and Nonlinear Fracture Mechanics also called Elastic Plastic Fracture Mechanics (NLFM or EPFM).

i. Linear Elastic Fracture Mechanics

A large field of Fracture mechanics uses concepts and theories in which Linear Elastic material behavior is an essential assumption. This is the case for Linear Elastic Fracture Mechanics (LEFM).

The basic assumption of the Linear Elastic Fracture Mechanics (LEFM) is that the size of Fracture Process Zone that is found beyond the crack tip is relatively small compared to the structure dimensions. Sometimes it is also called Small Scale Yielding (SSY).

It is also identified in its sharp cracks. This type of failure mechanics works well for those materials where the crack initiation load and the failure load is almost similar like those of most metals. The

global stress strain response of the material is linear and elastic. The basic formulation is based on energy balance.

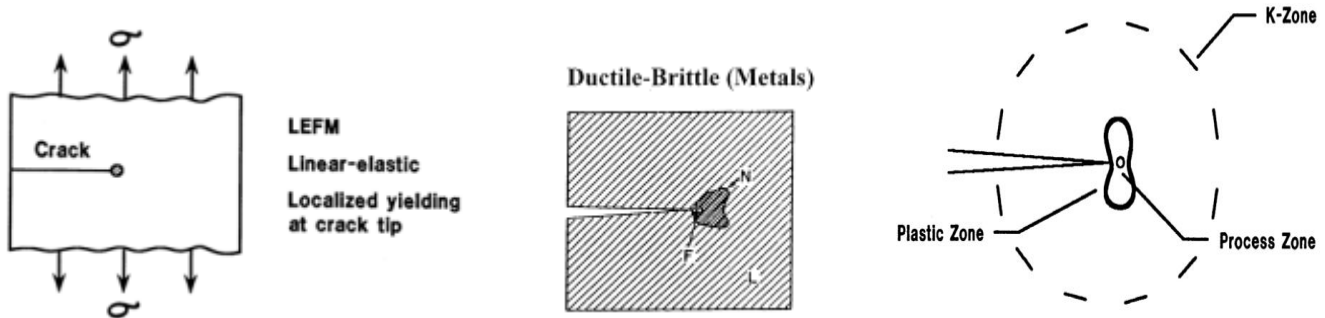


Figure 2. 7: crack tip variables for Sharp crack, [6]

In the above figures, the Fracture Process Zone is very small compared to the structure dimensions. F means area of Fracture Process Zone, N means area of nonlinear zone and L means part of the structure in the linear state. It is clear that most of the material cross-section is in the linear state so it is best to implement the LEFM.

All LEFM applies to sharp cracks in Elastic bodies. It is rational to apply this Fracture Mechanics for any material as long as the material is in the linear state and for the regions far away from the sharp crack tips, Implementation of LEFM near sharp crack leads to the predictions of infinite stress at crack tip. However, materials have finite stress capacity. The LEFM fails at molecular level or around the crack tip.

Literatures proposed some analytical tools to predict the Fracture Mechanics, which are based on the assumption of the linear elastic behavior of material. In the so called Linear Elastic Fracture Mechanics (LEFM), prediction of crack growth is based on the energy balance. Griffith states “crack growth will occur, when there is enough energy available to generate new crack surface.” The “energy release rate” is an essential quantity in energy balance criteria. The resulting crack growth criterion is referred to as being “global”, because a rather volume of material is considered. The crack growth criterion can also be based on the stress state at the crack tip. This stress field can be determined in several cases through an analytical approach.

It is characterized by the definition of the “stress intensity factor” (SIF). Stress intensity factor K : characterizes the stresses, strains and displacement fields near the crack tip, it is local parameter.

The crack growth criterion can also be based on the stress state at the crack tip. This stress field can be determined analytically. The resulting crack growth criterion is referred to as local, because attention is focused at a small material volume at the crack tip.

Assumption of linear elastic material behavior leads to infinite stresses at the crack tip. In reality this is obviously not possible: plastic deformation will occur in the crack tip region. Using yield criteria (Von Mises, Tresca), the crack tip plastic zone can be determined. When this zone is small enough (Small Scale Yielding, SSY), LEFM concepts can be used.

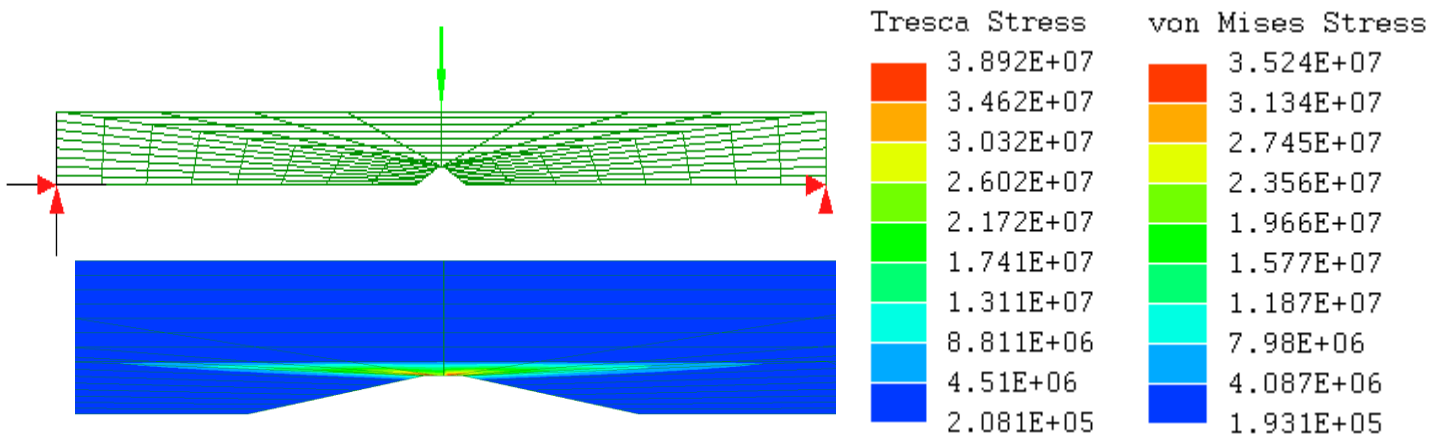


Figure 2. 8: Response of three point bend specimens with initial crack length a_0

When the global stress-strain response of the body is linear and elastic (LEFM), the elastic energy release rate, G , and the stress intensity factor can be used for characterizing cracks in structures.

Recall that the LEFM applies to sharp cracks, the assumption of sharp cracks, however, leads to the prediction of infinite stresses at the crack tip. On the other hand, stresses in real materials are finite because the crack tip radius is finite. In addition, inelastic deformation, e.g., plasticity in metals or damage in concrete, results in further reduction of crack tip stresses. These reasons cause modification of the LEFM to account for the crack tip yielding.

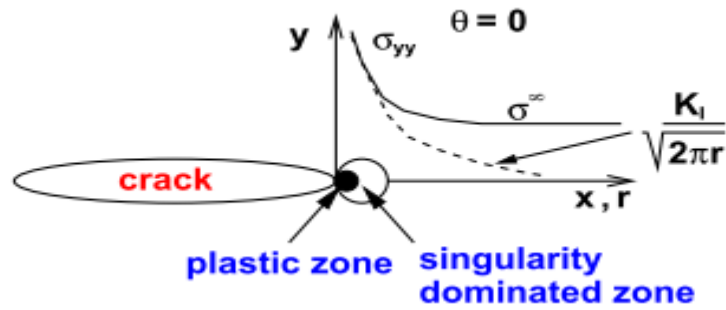


Figure 2. 9 : Crack tip stress conditions, [7]

If the plastic zone at the tip is sufficiently small (confined within the singularity dominated zone) there are two simple approaches available that provide correction to LEFM

A). The Irwin approach

First order estimates of the plastic zone

$$\sigma_{xx} = \sigma_{yy} = \frac{K_I}{\sqrt{2\pi r}} \quad \text{Solve for } r$$

$$r_y = \frac{1}{2\pi} \left(\frac{K_I}{\sigma_{ys}} \right)^2 \quad (2.7)$$

Analysis is based on elastic crack tip analysis

Second order estimates of plastic zones, when the yielding occurs the stress must be redistribute ahead of crack tip to satisfy equilibrium

$$\sigma_{ys} * r_p = \int_0^{r_y} \sigma_{yy} dr = \int_0^{r_y} \frac{K}{\sqrt{2\pi r}} dr$$

$$r_p = \frac{1}{\pi} \left(\frac{K_I}{\sigma_{ys}} \right)^2 = 2r_y \quad (2.8)$$

This is twice as much as values of first order estimates.

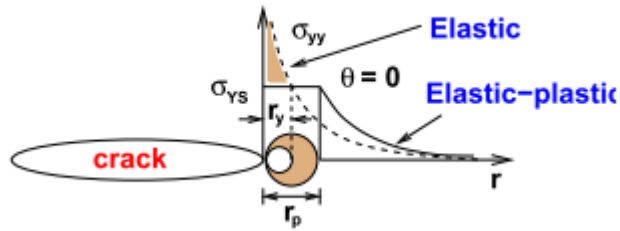


Figure 2. 10 : Crack tip radius for elastic and plastic zone, [4]

B). The strip yield model (suitable for polymers)

The strip yield model was first proposed by Dugdale and Barenblatt. They assumed a long slender plastic zone at the crack tip in non-hardening material in plane stress. This model is a classical application of the principle of superposition as it approximates the elastic-plastic behavior by superimposing two elastic solutions: a through crack under remote tension and a through crack with closure stresses at the tip.

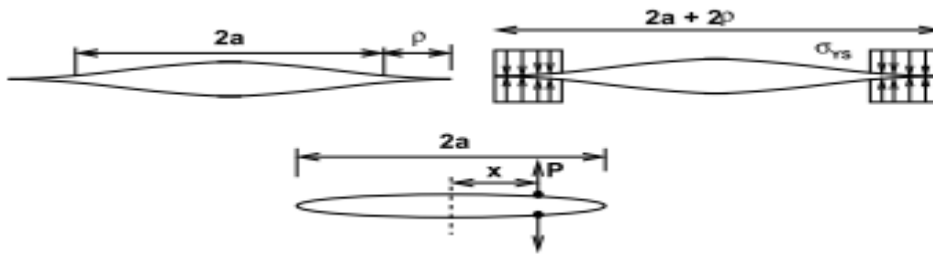


Figure 2. 11: Stress conditions causing opening and closing of crack tip, [2]

Since the stresses at the strip yield zone are finite, there cannot be a singularity at the crack tip (the stress intensity factor at the tip of plastic zone must be equal to zero). Thus the plastic zone length ρ is found from the condition that the stress intensity factors from the remote tension and closure stress cancel one another.

To proceed, consider first a through crack in an infinite plate loaded by a normal force P applied at a distance x from the center line of the crack. The stress intensities for the two crack tips are then give by

$$K_{+a} = \frac{P}{\sqrt{\pi a}} \sqrt{\frac{a+x}{a-x}} \quad K_{-a} = \frac{P}{\sqrt{\pi a}} \sqrt{\frac{a-x}{a+x}}$$

If the closure stress is σ_{ys} acts through a distances dx , the force developed due the closure stress

$$P = \sigma_{ys} dx$$

$$K_{closure} = \frac{\sigma_{ys}}{\sqrt{\pi a + \rho}} \int_a^{a+\rho} \left[\sqrt{\frac{a + \rho + x}{a + \rho - x}} + \sqrt{\frac{a + \rho - x}{a + \rho + x}} \right] dx$$

Solving the integral

$$K_{closure} = -2 * \sigma_{ys} \sqrt{\frac{a + \rho}{\pi}} \cos^{-1} \left(\frac{a}{a + \rho} \right)$$

The SIF for the remote stress is given by

$$K_{\sigma} = \sigma \sqrt{\pi a + \rho}$$

For the crack tip stress to be finite $K_{\sigma} = K_{closure}$

After simplifications

$$\frac{a}{a + \rho} = \cos \left(\frac{\pi \sigma}{2 \sigma_{ys}} \right)$$

Using the Taylor series for cosine functions where

$$\cos x = 1 - \frac{x^2}{2!} + \frac{x^4}{4!} - \frac{x^6}{6!} + \frac{x^8}{8!} + \dots$$

Using the same analogy

$$\cos \left(\frac{\pi \sigma}{2 \sigma_{ys}} \right) = 1 - \frac{\left(\frac{\pi \sigma}{2 \sigma_{ys}} \right)^2}{2!} + \frac{\left(\frac{\pi \sigma}{2 \sigma_{ys}} \right)^4}{4!} - \frac{\left(\frac{\pi \sigma}{2 \sigma_{ys}} \right)^6}{6!} + \frac{\left(\frac{\pi \sigma}{2 \sigma_{ys}} \right)^8}{8!}$$

If only two terms are taken and the rest are neglected and solve for plastic zone size gives

$$\rho = \frac{\pi^2 \sigma^2 a}{2 \sigma_{ys}} = \frac{1}{\pi} \left(\frac{K_I}{\sigma_{ys}} \right)^2 \quad (2.9)$$

Irwin plastic zone correction focused mainly on using effective crack length. However Dugdale focused on the ideas that stress at the elastic plastic boundary is not singular.

ii. Nonlinear Fracture Mechanics (Elastic-Plastic FM)

In many cases it is found that LEFM based criteria is either: too conservative and expensive as it does not account for plastification at the crack tip, and/or invalid based on calculations of r_p where LEFM assumptions are checked. Thus, in those cases where LEFM is not applicable, an alternative criteria for crack growth in Elasto Plastic Fracture Mechanics (EPFM) is sought.

LEFM is only valid as long as nonlinear material behavior is confined to a small region surrounding the crack tip. There are many materials, however, for which the applicability of LEFM is impossible or at least suspicious. Therefore, an alternative fracture mechanics model is required.

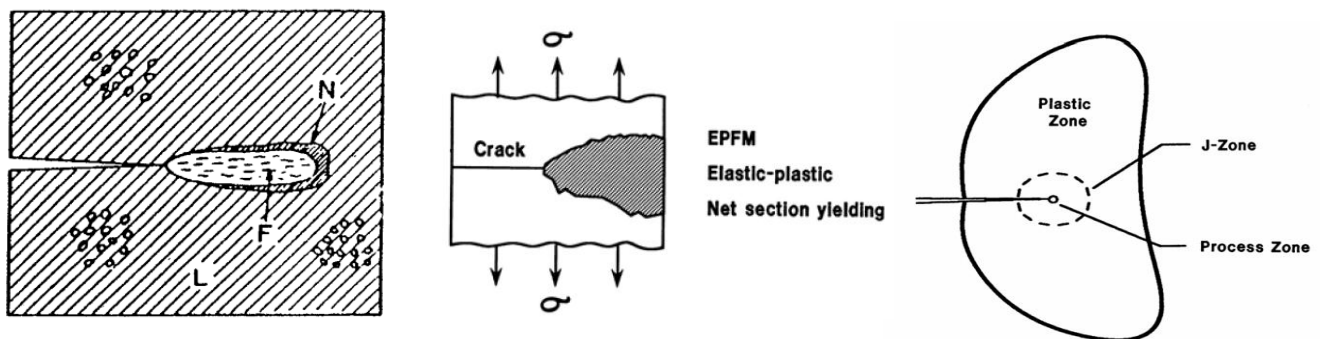


Figure 2. 12 : The fracture Process Zone developed beyond the crack is large enough to be considered, [6]

Elastic-plastic fracture mechanics applies to materials that exhibit time-independent, nonlinear behavior (plastic deformation).

The various stages of ductile fracture:

- ❖ Blunting of an initially sharp crack: Under LEFM assumptions, the crack tip opening displacement (CTOD) is zero, however in elasto-plastic material due to blunting it is different from zero.
- ❖ Crack initiation: Slow (stable) crack growth and Unstable crack growth

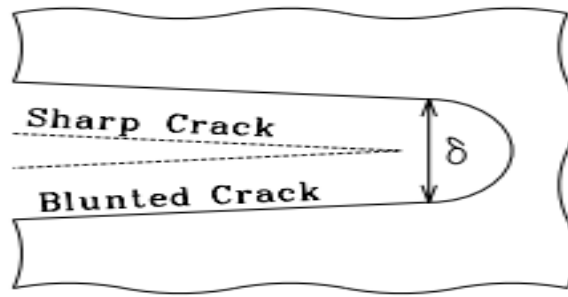


Figure 2.13: Blunted crack beyond the sharp crack, [5]

There are two parameters characterizing the nonlinear behavior at the crack tip:

- a. CTOD - crack tip opening displacement
- b. J counter integral

Critical values of CTOD and J give nearly size-independent measures of fracture toughness, even for relatively large amount of crack tip plasticity. But there are still limits to the applicability of J and CTOD, but these limit are much less restrictive than the validity requirements of LEFM, [5].

- a. Crack-tip opening displacement (CTOD)

In LEFM the displacement of material points in the region around the crack tip can be calculated. With the crack along the x-axis, the displacement u_y in y-direction is known as a function of r (distance) and θ (angle), both for plane stress and for plane strain.

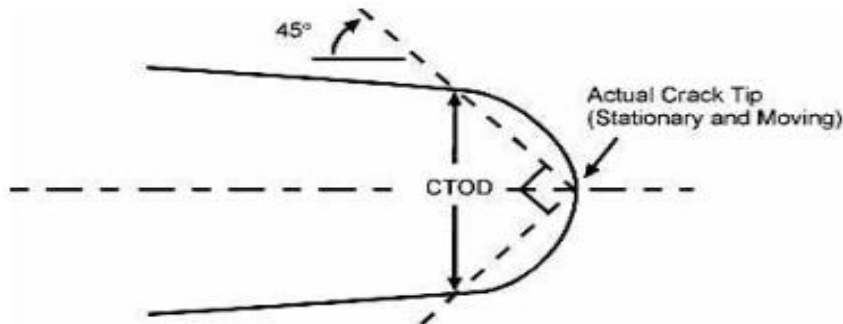


Figure 2. 14: Shows crack tip opening displacement [5]

The displacement of points at the upper crack surface results for $\theta = \pi$ and can be expressed in the coordinate x, by taking $r = a - x$, where, a is the half crack length. The origin of this xy-coordinate system is at the crack center. The crack opening displacement (COD) δ is two times this displacement.

It is obvious that the opening at the crack tip (CTOD), δ_t , is zero.

$$v_y = \frac{K_I}{2\mu} \sqrt{\frac{r}{2\pi}} \sin \frac{\theta}{2} \left[k + 1 - 2 \cos^2 \frac{\theta}{2} \right]$$

For crack plane $\theta = \pi$ and $r = a - x$

$$v_y = \frac{1 + \mu}{E} \frac{1 + k}{2} \sqrt{2a(a - x)} \frac{\sigma}{2}$$

COD = Crack Opening Displacement = δ_t

$$\delta_t = 2v_y = \frac{1 + \mu}{E} \frac{1 + k}{2} \sigma \sqrt{2a(a - x)} \quad (2.10)$$

Irwin and Dugdale both proposed different theories in the determinations of CTOD.

b. J-CONTOUR INTEGRAL

Rice presented a path-independent contour integral of analysis of cracks and showed that the value of this integral, called J, is equal to the energy release rate in a nonlinear elastic body that contains crack. Hutchinson and also Rice and Rosengren further showed that J uniquely characterizes crack tip stresses and strains in nonlinear material. Thus, the J integral can be viewed as both an energy parameter and a stress intensity parameter.

Comparisons of Linear and Nonlinear Fracture Mechanics

Linear Elastic Fracture Mechanics assumes that the material behaves in brittle manner and local parameter, stress intensity factor, can be used as valid fracture index. In this Fracture Mechanics, the plastic zone in the vicinity of the crack is about one-tenth of the initial crack length. However, if there is large scale yielding in the vicinity of the crack tip, another form of Fracture Mechanics called Non Linear Fracture Mechanics which is also called Elastic Plastic Fracture Mechanics should be used. In the Elastic Plastic Fracture Mechanics, There are two important Fracture parameters: The J-integral and Crack Tip Opening Displacement for handling the problem of large scale yielding.

Table 2. 1: Applicability of EPFM and LEFM

Elastic Plastic Fracture Mechanics	Linear Elastic Fracture Mechanics
Beyond small-scale yielding	Small-scale yielding applies
Lower strength materials	High strength materials
Tough, ductile materials	Brittle materials
Small thickness	Large thickness
Plane stress	Plane strain
High temperatures	Low temperatures
Slow loading rates	High loading rates

2.3 Cracks in Reinforced Concrete Structures

Members such as beams and slabs which are subjected to bending moment will develop flexural cracks when the stress in the tension zones exceeds the bending strength of plain concrete. From experience, crack extends commonly from tension face to the location of neutral axis of the cross section.

Cracking occurs in concrete member when the stress in concrete reaches the tensile strength, f_{ct} . The value of f_{ct} depends on several parameters. Choice of the appropriate values of f_{ct} is the first difficulty in the analysis of cracks. It was believed that the most important factor for controlling flexural crack is the magnitude of the strain in the reinforcing steel.

Control of strain in the reinforcing steel is believed to be the most effective means to limit the crack width. Other factors which have influence on the crack width are concrete cover, size of the reinforcing steel and distribution of reinforcing steel in tension zone. However it is difficult to predict the number and width of flexural cracks because of the complex process those are involved. As a result there is no uniform approach for estimating these quantities and various design codes use different techniques.

Cracks in Reinforced Concrete elements can be caused by force induced and displacement induced cracking. Provision of bonded reinforcement of sufficient magnitude and appropriate detailing can effectively limit the crack width. However size effect should come in to consideration before any conclusion is made. Some of the parameters which are used in crack width calculation are mean crack spacing (S_{rm}) and coefficient used to account for the additional stiffness which concrete in tension provide.

2.3.1 Variation of Tensile Strength of Concrete

The tensile strength of concrete may be subjected to large variation due to many reasons. One of the most common reason for the variation in strength is environmental effect. However, the variation caused by size effect is not captured well.

In most Reinforced Concrete structures analysis and design Hand Books, Upper ($f_{ctk,max}$) and lower values ($f_{ctk,min}$) of characteristic axial tensile strength with $f_{ctk,0}=10\text{Mpa}$.

$$f_{ctk,min} = 0.95 \left(\frac{f_{ck}}{f_{ctk,0}} \right)^{\frac{2}{3}} \quad \text{And} \quad f_{ctk,max} = 1.85 \left(\frac{f_{ck}}{f_{ctk,0}} \right)^{\frac{2}{3}} \quad (2.11)$$

Note that the tensile strength is independent of size. This means size effect is not yet considered.

2.3.2 Code Provision of Cracks

EBCS2, 1995.

Our building code discuss the issue of cracks under the serviceability states by different mechanisms. The code states that there are different source for cracks and there are some limitations regarding the limit state of crack formation and the limit states of crack width. But there is nothing which states about crack propagation.

The code states that creep and ambient conditions can cause cracks in concrete structures and the cracks are related with the characteristic compressive strength. The code states that when the issues of cracks needs to be considered, there are some issues which should be discussed along with crack. One of the most common is the amount of reinforcement bars in concrete. Another issue is the nature of stress distribution in the section.

Limit states of crack formation

According to our code, crack will be formed as long as the tensile stress caused by load exceeds the prescribed values in code. For flexure type of loading, the cracking tensile strength is about $1.7f_{ctk}$ and for direct tension it will be about f_{ctk} .

Limit States of crack width

Cracks due to flexure

$$\begin{aligned}w_k &= 1.7w_m \\w_m &= s_{rm}\varepsilon_{sm} \\s_{rm} &= 50 + 0.25k_1k_2 \frac{\phi}{\rho_r}\end{aligned}\tag{2.12}$$

Where

w_k = characteristic crack width w_m = mean crack width s_{rm} = average distance between cracks

ε_{sm} = mean strain of the reinforcement considering the contribution of concrete in tension

ϕ = bar diameter, k_1 = bond parameter, 0.8 for deformed bars and 1 for plain bars

k_2 = accounts for stress diagram, 0.5 for bending, 1 for pure tension and $\frac{\varepsilon_{c1} + \varepsilon_{c2}}{2}$ for bending with tension

ε_{c1} And ε_{c2} larger and smaller concrete strains, below the neutral axis of the cracked section

$$\rho_r = \frac{A_s}{A_{c,eff}}$$

A_s area of reinforcement bars and $A_{c,ef}$ effective embedment zone

Eurocode 2/ EN 1992

Eurocode 2 states that cracks can be caused by direct loading or restraining of imposed deformation. Crack can also be caused by plastic shrinkage or expansive chemical reactions within the hardened concrete. Like Our building EBCS2, 1995 Eurocode states that the amount of reinforcement in concrete can play great role when the issue of cracks comes in to consideration. In addition, only the limit states of crack formation and crack width are discussed but the idea of crack propagation is still out of consideration.

According to Eurocode 2, if the depth is less than 200mm, effect crack can be neglected and no need to control.

Limit States if crack width

$$w_k = s_{r,max} (\varepsilon_{sm} - \varepsilon_{cm}) \quad (2.13)$$

Where $s_{r,max}$ is maximum crack spacing

$$s_{r,max} = 3.4c + 0.425k_1k_2 \frac{A_s}{A_{c,eff}}$$

Where

c = concrete cover

$$k_1 = \begin{cases} 0.8 & \text{for deformed bar} \\ 1 & \text{for plain bar} \end{cases} \quad (\varepsilon_{sm} - \varepsilon_{cm}) = \frac{\sigma_s + k_t \frac{f_{ct,eff}}{\rho_{p,eff}} (1 + \alpha_e \rho_{p,eff})}{E_s}$$

$$k_2 = \begin{cases} 0.5 & \text{for bending} \\ 1 & \text{for tension} \end{cases}$$

Where σ_s is tensile stress in tension reinforcement assuming cracked section

$$\alpha_e = \frac{E_s}{E_{cm}} \quad \text{and} \quad \rho_{p,eff} = \frac{A_s}{A_{c,eff}}$$

ACI

ACI 2009 manuals for concrete structures dictates that cracks are function of the bond stress that develop between the concrete and reinforcement bars. Real life experiences shows that crack can exist even before the first loading due to shrinkage. In well-designed beam, the cracks are hairline types with very small width and large in numbers. Most equations used for crack width determinations have been used to predict the maximum crack width. Usually 90% of the crack width in members are below the calculated values. However, isolated cracks exceeding twice the computed width can occur sometimes.

ACI also states that stress in the reinforcement bars, concrete cover, distributions of reinforcement bars in the tension zone and diameter of the bars have significant effect on crack width.

By considering the major factors which can possibly affect the crack width, ACI committee 224 recommends the following flexural crack-width formula, which is based on the Gergely-Lutz equation:

$$w = 55.88\beta\varepsilon_s\sqrt[3]{d_c A} \quad (2.14)$$

Where

w = most probable crack width [mm]

β = ratio of distance between neutral axis and tension face to distance between neutral axis and centroid of reinforcing steel

ε_s = strain in the reinforcement due to applied load

d_c = concrete cover from tension face to center of reinforcing bars.[mm]

A_c = area of concrete symmetric with reinforcing bars divided by the number of bars [mm²]

The ACI Code (ACI 318-89) does not include a formula to compute explicitly crack width under the service load. However, it uses Z-value to control cracks indirectly:

$$Z = f_s\sqrt[3]{d_c A} \quad (2.15)$$

The ACI code places limits on the Z-value as a means to control crack width. This emphasis that the strain in the reinforcing bars plays critical role in crack width and it is rational to use this rather than the direct prediction of crack width which is very susceptible to uncertainty. However, using the Z-value in crack width control, spacing of the cracks cannot be captured.

CEB/FIP Approach

The CEB/FIP Model Code 1990 (CEB 1990) for concrete structures uses an approach for crack control that differs from the ACI approach. The CEB/FIP technique considers the mechanism of stress transfer between the concrete and reinforcement to estimate crack width and spacing.

Prior to cracking, tensile load applied to the beam causes equal strains in the concrete and steel. The strains increase with increasing load until the strain capacity of the concrete is reached, at which cracks develop in the concrete. At the crack locations, the applied tensile load is resisted entirely by the steel. Adjacent to the cracks, there is slip between the concrete and steel, and this slip is the fundamental factor controlling the crack width.

The slip causes transfer of some of the force in the steel to the concrete by means of interracial stress (called bond stress) acting on the perimeter of the bar. Therefore, the concrete between the cracks participates in carrying the tensile force. The bond-slip mechanism causes the strains in the concrete and steel to have a periodic variation along the length of the member. At a crack, the steel strain is maximum and the concrete strain is zero. In between cracks, the steel strain is minimum and the concrete strain is maximum. If, under increasing load, the concrete strain reaches the limiting tensile strain, an intermediate crack forms between two previously formed cracks.

Crack width is related to the distance over which slip occurs and to the difference between the rebar and concrete strains in the slip zones on either sides of the crack.

$$w_k = l_{s,max} (\varepsilon_{sm} - \varepsilon_{cm} - \varepsilon_{cs}) \quad (2.16)$$

Where, w_k characteristic crack width

$l_{s,max}$ = maximum distance over which slip between concrete and rebar occurs

ε_{sm} = Average rebar strain within $l_{s,max}$

ε_{cm} = Average concrete strain within $l_{s,max}$

ε_{cs} = Concrete shrinkage strain

Approximately

$$l_{s,max} = \frac{\phi}{3.6\rho_{s,eff}}$$

Where ϕ = bar diameter $\rho_{s,eff}$ = area of rebars divided by effective area of concrete in tension

In the CEB/FIP approach, the bond stress is assumed to be uniform over the slip distance and equal to 1.8 times the concrete tensile strength. According to this bond-slip model, intermediate cracks can occur only when the spacing between cracks exceeds $l_{s,max}$. Thus crack spacing will range from $l_{s,max}$ to $0.5 l_{s,max}$.

To evaluate crack width, it is necessary to evaluate the difference between the average steel and average concrete strains within the slip zone. This difference is approximated by the following (CEB 1990):

$$\varepsilon_{sm} - \varepsilon_{cm} = \varepsilon_{s2} - \beta \varepsilon_{sr2}$$

Where

ε_{s2} = steel strain at location of crack under service load

ε_{sr2} = steel strain at location of crack under load that causes cracking of the effective concrete area

β =empirical factor to assess average strain within $l_{s,max}$ ($\beta = 0.6$ for short-term loading and $\beta = 0.38$ for long-term loading).

2.3.3 Finite Element Analysis of Cracks

Finite Element Analysis is one of the numerical methods to obtain approximate solutions to many of the Fracture Mechanics problems. To briefly explain the methodology consider 2D stress analysis. The displacement variable $\phi^c(x, y)$ in each element domain can be defined as

$$\phi^c(x, y) = a_1 + a_2x + a_3y + a_4xy + a_5x^2 + a_6y^2 + \dots$$

In terms of nodal values

$$\phi^c(x, y) = N_1(x, y) \phi_1 + N_2(x, y) \phi_2 + N_3(x, y) \phi_3 + N_4(x, y) \phi_4 + \dots$$

For triangular elements with nodes (i, j, k) at the three vertices, the displacements (U, V) within the elements

$$U_{x,y} = N_1(x,y)u_1 + N_2(x,y)u_2 + N_3(x,y)u_3$$

$$V_{x,y} = N_1(x,y)v_1 + N_2(x,y)v_2 + N_3(x,y)v_3$$

Strain components

$$\varepsilon_x = \frac{\partial u}{\partial x} \quad \varepsilon_y = \frac{\partial v}{\partial y} \quad \varepsilon_{xy} = \frac{\partial v}{\partial x} + \frac{\partial u}{\partial y}$$

The above relation can be expressed in matrix form as shown below

$$\begin{bmatrix} \varepsilon_x \\ \varepsilon_y \\ \gamma_{xy} \end{bmatrix} = \begin{bmatrix} \frac{\partial N_1}{\partial x} & 0 & \frac{\partial N_1}{\partial x} & 0 & \frac{\partial N_j}{\partial x} & 0 \\ 0 & \frac{\partial N_1}{\partial y} & 0 & \frac{\partial N_j}{\partial y} & 0 & \frac{\partial N_k}{\partial y} \\ \frac{\partial N_i}{\partial y} & \frac{\partial N_i}{\partial x} & \frac{\partial N_j}{\partial x} & \frac{\partial N_i}{\partial x} & \frac{\partial N_k}{\partial x} & \frac{\partial N_k}{\partial x} \end{bmatrix} \begin{bmatrix} u_1 \\ v_1 \\ u_2 \\ v_2 \\ u_3 \\ v_3 \end{bmatrix}$$

In compact form $\varepsilon = \mathbf{B} [\mathbf{U}^e]$

The stress strain relation, also known as constitutive relation, for linear isotropic plane stress

$$\begin{bmatrix} \sigma_x \\ \sigma_y \\ \tau_{xy} \end{bmatrix} = \frac{E}{1-\nu^2} \begin{bmatrix} 1 & \nu & 0 \\ \nu & 1 & 0 \\ 0 & 0 & \frac{1-\nu}{2} \end{bmatrix} \begin{bmatrix} \varepsilon_x \\ \varepsilon_y \\ \gamma_{xy} \end{bmatrix}$$

Or in compact Form $\sigma = \mathbf{D} \varepsilon$

By using minimization of the total potential energy, the element stiffness matrix will be

$$[\mathbf{k}^e] = \int \mathbf{B}^T \mathbf{D} \mathbf{B} \, dA$$

Where,

h is thickness of the material.

The element stiffness matrix can be assembled to form the global stiffness matrix [K]. Thus finally FE equation can be written as

$$K U = P$$

Where,

[P] = applied nodal loads

[U] = Nodal displacement and [K] = element Stiffness matrix

There are some direct methods to determine Fracture Mechanics parameters for crack analysis. The stress-strain fields in 2D crack problems can be determined in general by using 3-node, 6-node triangular elements, 4-noded quadrilateral or 8- node isoperimetric elements.

Making use of expressions for the displacements and stress near the crack tip

$$\begin{aligned} u_i &= K_I \sqrt{\frac{r}{2\pi}} f(\theta) \\ \sigma_{ij} &= \frac{K_I}{\sqrt{2\pi r}} g_{ij} \theta \end{aligned} \quad (2.17)$$

For mode I cracking

$$\begin{bmatrix} \sigma_x \\ \sigma_y \\ \tau_{xy} \end{bmatrix} = \frac{K_I}{\sqrt{2\pi r}} \cos \frac{\theta}{2} \begin{bmatrix} 1 - \sin \frac{\theta}{2} \sin \frac{3\theta}{2} \\ 1 + \sin \frac{\theta}{2} \sin \frac{3\theta}{2} \\ \sin \frac{\theta}{2} \cos \frac{3\theta}{2} \end{bmatrix}$$

And the displacement field for plane strain condition

$$\begin{bmatrix} \mathbf{U} \\ \mathbf{V} \end{bmatrix} = 2 \frac{1+\nu}{E} \frac{K_I}{\sqrt{2\pi r}} \begin{bmatrix} \cos \frac{\theta}{2} \left(1 - 2\nu + \sin^2 \frac{\theta}{2} \right) \\ \sin \frac{\theta}{2} \left(2 - 2\nu - \cos^2 \frac{\theta}{2} \right) \end{bmatrix}$$

K_I can be calculated from the stress field

$$K_I = \sigma_{ij} \frac{\sqrt{2\pi r}}{g_{ij} \theta}$$

Or from the known displacements

$$K_I = \sigma_{ij} \frac{\sqrt{2\pi}}{f_{ij} \theta \sqrt{r}}$$

In crack growth criteria of LEFM and NLFM, a crack growth parameter has to be calculated and compared to the critical value. Crack parameters G, K, CTOD and J integral can be calculated analytically but this is only possible with great deal of mathematical effort.

Special elements

Refinements at the crack tip mesh to get better result may result the solution to be divergent. One possible solution for such type of problem is to change the interpolation function of the element. This element is called enriched elements which is used for crack tip analysis. Another method is to use hybrid elements where stress are unknown nodal variables.

In 1976, Barsoum used quarter point elements to determine the stress singularity at the crack tip. They are 8-noded quadrilateral and 6-noded triangular elements where two mid side points are positioned towards one corner node such that they divide the sides in then ratio 1:3.

Some examples of quarter point elements

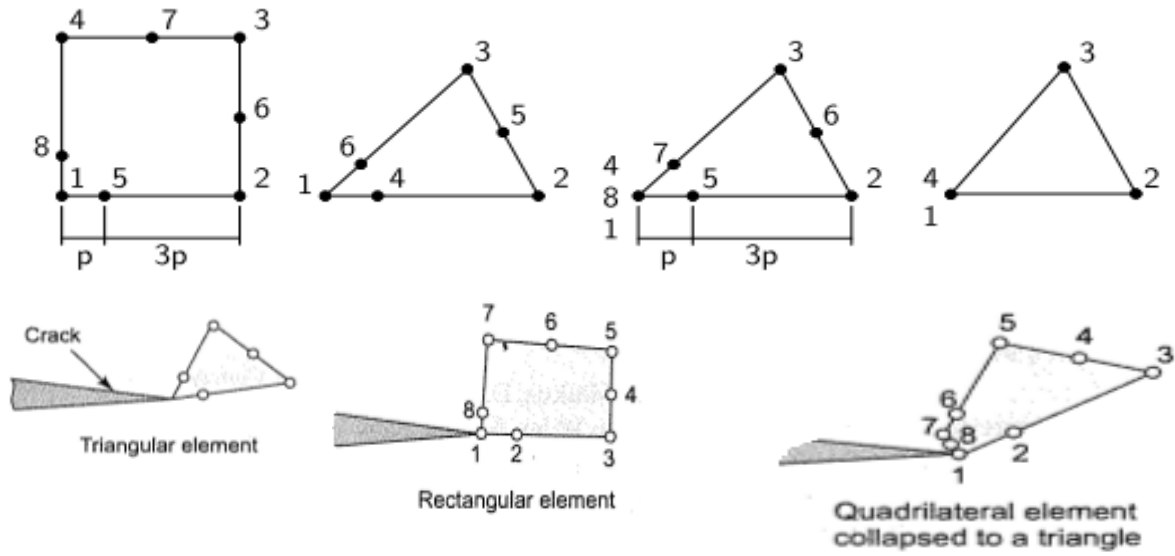


Figure 2. 15: Quarter points and collapsed elements, [5]

2.3.4 Crack tip stress and strain

Even though the actual stress-strain state near the crack tip is in triaxial state, many researchers in the area including Irwin and Dugdale assumed that the stress-strain state near the crack tip is uniaxial in the determination of the plastic zone.

By adopting 2D basic concepts, cracked structures subjected to external loads can be properly analyzed and closed form solution can be obtained. Researchers such as Westergaard, Irwin, Sneddon and Williams are among the first to publish the closed form solutions.

These researchers shows that once the polar coordinates at the crack tip is defined, the stress-strain state at any radius and angle can be expressed as shown below

$$\sigma_{ij} = \left(\frac{K}{\sqrt{r}} \right) f_{ij}(\theta) + \sum_{m=0}^n A_m r^{m/2} g_{ij}^m(\theta)$$

Where,

σ_{ij} is a stress tensor , K is a constant (SIF), and
 f_{ij} is dimensionless function of θ

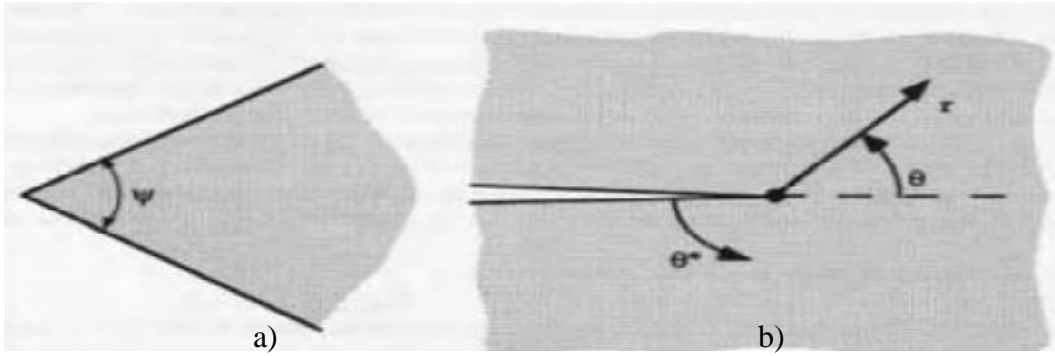


Figure 2. 16: a) Plate corner with included angle; b) Special case of sharp Crack, [5]

Stress-strain state at the crack tip can be analyzed by variety of methods. Two of the most common are Williams and Westergaard Approaches. The basic idea of Williams approach is considering the local stress fields under generalized in plane loading while Westergaard consider the connection of local fields to global boundary condition in certain configuration.

Williams Approaches:

Williams actually began by considering the stress-strain state at the corner of the plate with various boundary condition and included angles. From Williams works, crack is defined as special case of plate with corner angle of 2π and where the surface are traction free.

Williams postulated the following stress function

$$\Phi = r^{\lambda+1} * \phi(\theta^*), \lambda$$

$$\Phi = r^{\lambda+1} [C_1 \sin(\lambda+1)\theta^* + C_2 \cos(\lambda+1)\theta^* + C_3 \sin(\lambda-1)\theta^* + C_4 \cos(\lambda-1)\theta^*]$$

Where

C_1, C_2, C_3 and C_4 are non zero constants, and θ^* are defined as shown in the figure below.

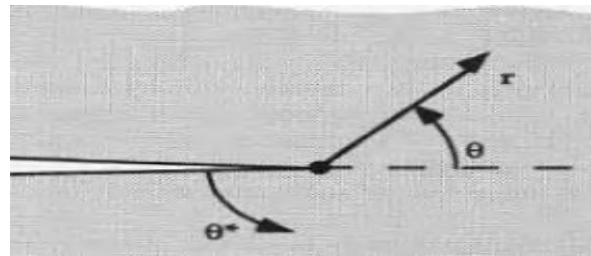


Figure 2. 17: Orientation of the crack plane, [5]

After simplification

$$\begin{aligned}\sigma_{rr} &= r^{\lambda-1} \left[F'' \theta^* + \lambda + 1 F \theta^* \right] \\ \sigma_{\theta\theta} &= r^{\lambda-1} \left[\lambda + 1 \lambda F \theta^* \right] \\ \tau_{r\theta} &= r^{\lambda-1} \left[-\lambda F' \theta^* \right]\end{aligned}$$

If the surface is traction free

$$\sigma_{\theta\theta} \big|_0 = \sigma_{\theta\theta} \big|_{2\pi} = \tau_{r\theta} \big|_0 = \tau_{r\theta} \big|_{2\pi} = 0$$

This implies that

$$F \big|_0 = F \big|_{2\pi} = F' \big|_0 = F' \big|_{2\pi} = 0$$

Assuming the constants to be nonzero where C_1, C_2, C_3 and $C_4 \neq 0$ to satisfy the boundary condition and solve for λ

$$\sin 2\pi\lambda = 0$$

$$\lambda = \frac{n}{2}$$

There are infinite number of λ which can satisfy the boundary conditions. In most general form

$$\Phi = \sum_{n=1}^N \left(r^{\frac{n}{2}+1} F \theta^*, \frac{n}{2} \right)$$

And the stresses are expressed as:

$$\sigma_{ij} = \frac{\Gamma \theta, -1/2}{\sqrt{r}} + \sum_{m=0}^m \left(r^{\frac{m}{2}} \Gamma \theta^*, m \right) \quad (2.18)$$

Where, Γ Function depends on F and its derivatives.

For crack tip, as r goes to zero, this shows the first term to be infinity while for the second term if $m=0$, it will be finite however if $m>0$, it will be zero. This shows that higher order terms are negligible around the crack tip.

The crack tip stress field for mode I loading can be expressed as follows by ignoring the higher order terms.

$$\begin{bmatrix} \sigma_{rr} \\ \sigma_{\theta\theta} \\ \tau_{r\theta} \end{bmatrix} = \frac{K_I}{\sqrt{2\pi r}} \begin{bmatrix} \frac{5}{4} \cos\left(\frac{\theta}{2}\right) - \frac{1}{4} \cos\left(\frac{3\theta}{2}\right) \\ \frac{3}{4} \cos\left(\frac{\theta}{2}\right) + \frac{1}{4} \cos\left(\frac{3\theta}{2}\right) \\ \frac{1}{4} \sin\left(\frac{\theta}{2}\right) + \frac{1}{4} \sin\left(\frac{3\theta}{2}\right) \end{bmatrix}$$

For mode II loading, the stress field around the crack

$$\begin{bmatrix} \sigma_{rr} \\ \sigma_{\theta\theta} \\ \tau_{r\theta} \end{bmatrix} = \frac{K_{II}}{\sqrt{2\pi r}} \begin{bmatrix} -\frac{5}{4} \sin\left(\frac{\theta}{2}\right) + \frac{3}{4} \sin\left(\frac{3\theta}{2}\right) \\ -\frac{3}{4} \sin\left(\frac{\theta}{2}\right) - \frac{3}{4} \sin\left(\frac{3\theta}{2}\right) \\ \frac{1}{4} \cos\left(\frac{\theta}{2}\right) + \frac{3}{4} \cos\left(\frac{3\theta}{2}\right) \end{bmatrix}$$

Where K_I and K_{II} are stress intensity factors for Mode I and Mode II loading conditions. This parameters defines the amplitude of the stress singularity around the crack tip. As long as the crack is stationary, the stress and strain state increase in proportion to the stress intensity factor (K) (SIF). Previous work by researcher's shows that SIF (K) can be expressed Interms of the \sqrt{GE} expressions, where G is the fracture energy (Energy release rate) and E is modulus of elasticity.

Westergaard Approaches:

Westergaard shows that complex stress function $Z(z)$ can be used to solve certain limited problems where $Z z = x + iy$ where $I = \sqrt{-1}$.

Westergaard stress function

$$\Phi = \text{Re} \bar{Z} + y \text{Im} \bar{Z}$$

$$\bar{Z} = \frac{d\bar{Z}}{dz} \quad \text{and} \quad Z = \frac{dZ}{dz}$$

This shows that

$$\sigma_{xx} = \operatorname{Re} Z - y \operatorname{Im} Z' \quad (2.19)$$

$$\sigma_{yy} = \operatorname{Re} Z + y \operatorname{Im} Z' \quad (2.20)$$

$$\sigma_{xy} = -y \operatorname{Im} Z' \quad (2.21)$$

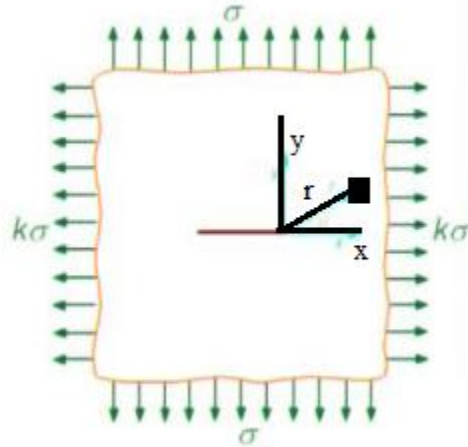


Figure 2. 18: Biaxial loading for Westergaard solution, [14]

From the above it is clear that the shear stress vanishes when $y = 0$, implying that the crack plane is principal plane. The original form of the Westergaard approaches is limited to certain types of Mode I crack problems. In the Westergaard approaches the local stress is related to the global stress and crack size.

2.3.5 Plastic crack- tip zone

Near the crack tip, the elastic stress intensity factors reaches to infinity which is impossible due to finite capacity of the material. In reality, the material yield before the stress reaches to infinity value and the elastic solution will no longer valid. Stress at crack tip is finite and some corrections regarding with this are already done by many researchers.

The zone where the singularity occurs is called Fracture Process Zone. And the size of the material has noticeable effect on the crack behavior. Occurrence of yielding can be tested by yielding criteria. From the different methods which are used for checking whether the material yields or not, two of the most familiars are Von Mises and Tresca Yield criteria are discussed below.

Both theories are formulated in terms of the principal stress σ_1 , σ_2 and σ_3 where σ_1 and σ_2 are in plane principal stress while σ_3 is out of plane stress. For the plane stress problems $\sigma_3 = 0$ and for plane strain problems, $\sigma_3 = \nu(\sigma_1 + \sigma_2)$ where ν Poisson's ratio of the material.

According to Von Mises, a specific criteria for yield is mainly depends on the amount of distortional elastic energy. But in Tresca, yielding occurs when the shear stress reaches at some maximum value.

For Von Mises

$$W^d = W_c^d$$

$$\sigma_1 - \sigma_2 \quad ^2 + \sigma_3 - \sigma_2 \quad ^2 + \sigma_1 - \sigma_3 \quad ^2 = 2\sigma_y^2$$

For plane stress where, $\sigma_3 = 0$, the plastic zone (r_p) after simplification

$$r_p = \frac{K_I^2}{4\pi\sigma_y^2} \left(1 + \cos\theta + \frac{3}{2} \sin^2\theta \right)$$

For plane strain where $\sigma_3 = 0$, the plastic zone r_p , after simplification

$$r_p = \frac{K_I^2}{4\pi\sigma_y^2} \left(1 - 2\nu \quad ^2 + 1 + \cos\theta + \frac{3}{2} \sin^2\theta \right)$$

For Tresca

$$\tau_{\max} = \tau_{\max c}$$

$$\sigma_{\max} - \sigma_{\min} = \sigma_y$$

For plane stress problems $\sigma_1 - \sigma_2 = \sigma_y$ since $\sigma_3 = 0$, After simplification, plastic zone size

r_p

$$r_p = \frac{K_I^2}{2\pi\sigma_y^2} \left(\cos\frac{\theta}{2} + \left| \cos\frac{\theta}{2} \sin\frac{\theta}{2} \right| \right)^2 \quad (2.22)$$

For plane strain condition

Condition 1 where $\sigma_1 > \sigma_2 > \sigma_3$

$$r_p = \frac{K_I^2}{2\pi\sigma_y^2} \left((1-2\nu) \cos \frac{\theta}{2} + \left| \cos \frac{\theta}{2} \sin \frac{\theta}{2} \right| \right)^2 \quad (2.23)$$

Condition 2 where $\sigma_1 > \sigma_3 > \sigma_2$

$$r_p = \frac{K_I^2}{2\pi\sigma_y^2} \sin^2 \theta \quad (2.24)$$

Stable and unstable crack propagation

Crack tip speed and its propagation mainly depends on the general energy balance. When crack is subjected to mode I load with δ , resulting from external load applied at the edges far away from the crack, the external work done will be zero when crack length changes.

Using energy balance

$$\frac{du_e}{da} - \frac{du_i}{da} = \frac{du_a}{da} + \frac{du_d}{da} + \frac{du_k}{da} \quad (2.25)$$

If the dissipated energy is assumed to be very small and enough to be ignored, all the available energy is going to be transformed in to surface energy and kinetic energy

$$\frac{du_e}{da} = 0 \quad \text{and} \quad \frac{du_d}{da} = 0$$

For central crack in large plate with unloaded Elliptical area

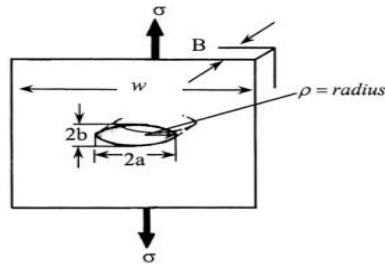


Figure 2. 19: Plate subjected to far field stress, [2]

Surface energy $U_a = 4ab\gamma_s$

$$\frac{dU_a}{da} = 4b\gamma_s$$

Internal energy $U_i = 2\pi a^2 b \frac{\sigma^2}{2E}$

$$\frac{dU_i}{da} = 2\pi ab \frac{\sigma^2}{2E}$$

Total kinetic energy $KE = \frac{1}{2} \rho * V * \left(\left(\frac{du_x}{dt} \right)^2 + \left(\frac{du_y}{dt} \right)^2 \right)$

Where, ρ is material density, V is material volume and $\left(\frac{du_x}{dt} \right)$ and $\left(\frac{du_y}{dt} \right)$ are the material velocity components. For constant thickness, b , $V = b dx dy$

$$KE = \frac{1}{2} \rho * b * \int \left(\left(\frac{du_x}{dt} \right)^2 + \left(\frac{du_y}{dt} \right)^2 \right) dx dy$$

For material velocity, $\left(\frac{du_x}{dt} \right) \ll \left(\frac{du_y}{dt} \right) = \frac{du_y}{dt} = \frac{du_y}{da} \frac{da}{dt} = \frac{du_y}{da} S$

Where, $S = \frac{da}{dt}$, crack speed.

For plane stress of u_y of crack face with $\theta = \pi$

$$\frac{du_k}{da} = \frac{1}{2} \rho S^2 b \iint \frac{d}{da} \left(\frac{du_y}{da} \right)^2 dx dy$$

For the given crack shape $u_y = 2\sqrt{2} \frac{\sigma}{E} \sqrt{a^2 - ax}$

Substitute the u_y in to the above integral $\frac{du_k}{da} = \frac{1}{2} \rho S^2 b \left(\frac{\sigma}{E} \right)^2 a K a$

Back to energy balance $\frac{2\pi a\sigma^2}{E} = 4\gamma_s + \frac{1}{2}\rho S^2 b \left(\frac{\sigma}{E}\right)^2 aK a$

Solve for crack speed S, $S = \sqrt{\frac{2\pi}{K} \left(1 - \frac{2\gamma_s E}{\pi a\sigma^2}\right) \frac{E}{\rho}}$

For $a_c = \frac{2\gamma E}{\pi\sigma^2}$ and $c = \sqrt{\frac{E}{\rho}}$

Finally, s will be

$$S = 0.38c \left(1 - \frac{a_c}{a}\right)^{\frac{1}{2}} \tag{2.26}$$

For $a \gg a_c$,

$$S = 0.38c$$

2.4 Section Capacity of Reinforced Concrete Elements

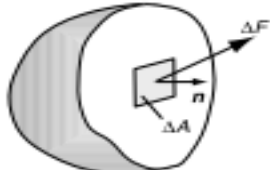
2.4.1 Stress and strain diagram

The subject of mechanics of materials involves analytical methods for determinations of the strength, stiffness and stability of the various members in structural system. The behavior of members depends on not only on the fundamental law that govern the equilibrium of force but also on mechanical characteristics of the material.

This mechanical characteristics comes from laboratory, where materials are tested under accurately known forces and their behavior is carefully observed and measured.

Reinforced Concrete Mechanical Characteristics

Stress: it is the intensity of Force acting on infinitesimal area of section. Mathematically this can be expressed as

$$\sigma = \lim_{\Delta A \rightarrow 0} \frac{\Delta F}{\Delta A} \tag{2.27}$$


The diagram shows a 3D perspective of a curved section body. A small square area element, labeled ΔA, is highlighted on the surface. A force vector, labeled ΔF, is shown acting on this area element, pointing away from the surface along a normal direction, which is also labeled 'n'.

Figure 2. 20: Section body, [14]

For the sake of simplicity these stress can be resolved in to two components, one is parallel the cross section and is called shear stress (S) and the other is perpendicular to the section and is called normal stress (N).

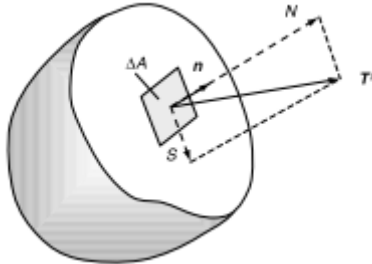


Figure 2. 21: Tractions decomposition, [14]

The state of the stress at any point can be described by using three components of stress on each three mutually perpendicular direction. This term is called stress tensor.

Matrix representation of the stress tensor

$$\sigma_{ij} = \begin{bmatrix} \sigma_{xx} & \tau_{xy} & \tau_{xz} \\ \tau_{yx} & \sigma_{yy} & \tau_{yz} \\ \tau_{zx} & \tau_{zy} & \sigma_{zz} \end{bmatrix}$$

To satisfy equilibrium of moment stress tensor is symmetric i.e. $\tau_{ij} = \tau_{ji}$

When the out of plane stress, stresses in the directions of $\sigma_{zz} = \tau_{yz} = \tau_{xz} = 0$ or when all elements in the 3rd column and 3rd rows are zeros, the 2D state is called plane stress problems. However, if $\epsilon_{zz} = \gamma_{yz} = \gamma_{xz} = 0$, it is called plane strain problems.

For plane stress problems if $\sigma_{zz} = 0$, Biaxial state of stress and if further $\sigma_{yy}=0$, it is called uniaxial state of stress.

When the stress are calculated in the original area of the member, they are referred as conventional or engineering stress. However, if the member cross sections are assumed to be the actual, the stress calculated is called true stress.

Strain

Any physical body responds to the loads in different mechanisms. When a member is subjected to a loading, P, extensions of member length will be inevitable as long as the load P increase. If the initial gage length is L_0 and final gage length after load increment is L, the elongation per unit gage length is

$$\varepsilon = \frac{L - L_0}{L_0} = \frac{\Delta L}{L_0}$$

ε is called normal strain.

However, if ε is very large compared to other case of small strains, Natural or True strain, $\bar{\varepsilon}$ better expressed the response.

Evaluate from L_0 to L

$$\bar{\varepsilon} = \ln(1 + \varepsilon) \quad (2.28)$$

Stress – Strain relation $\sigma - \varepsilon$

Stress –Strain relation shows how the material responds to loading under different scenario. Each material has its own Stress –Strain relation. However the Stress –Strain relation is very sensitive to different factors like those of size effect, internal Flaws and temperature changes. For the sake of simplicity most materials are assumed to be homogenous and isotropic. Materials with large strains without any significant stress increment are called Ductile Materials while those with inverse behaviors are called Brittle Materials. Another Types of Materials which exhibits intermediate behaviors are called quasi brittle Materials.

2.4.2 Code provisions on stress strain diagram

According to EBCS 2, 1995, the stress-strain diagram is expressed as follows

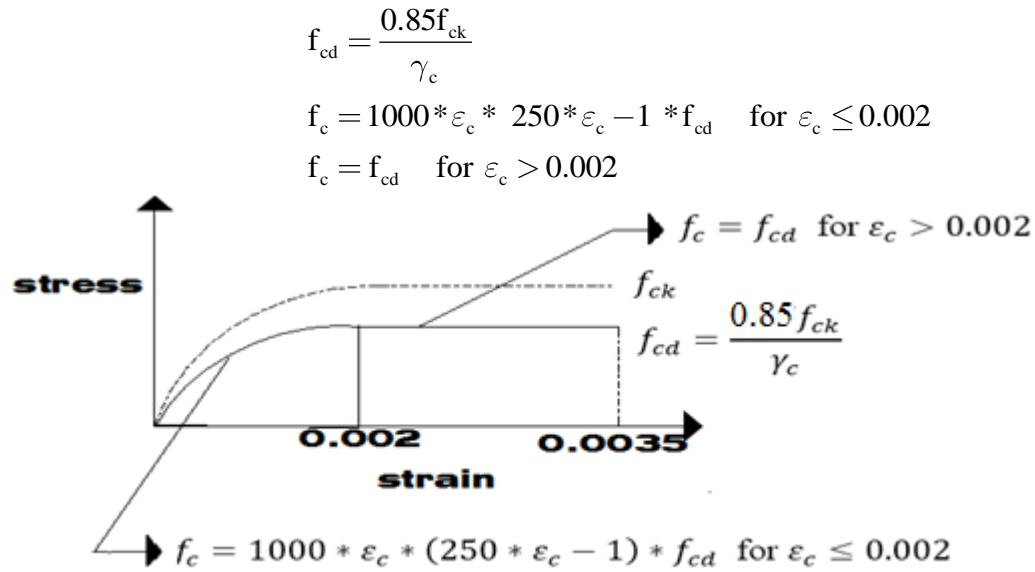


Figure 2. 22: EBCS 2, 1995 provision for stress-strain diagram for concrete under compression, [18]

Where

f_{ck} = characteristic compressive strength

ε_c = strain in the concrete

f_{cd} = design compressive strength

Note that the stress-strain diagram is independent of size.

Eurocode 2, 1994(EU 2, 1994)

Similar to EBCS 2, 1995, the Euro code 2, 1994 provide stress-strain diagram which is independent of size. However, Eurocode 2, 1994 provide two diagram for the analysis and design of concrete sections. One of the most common is the parabolic-rectangular diagram which is very similar to the EBCS 2, 1995. The second one is simplified one for the sake analysis and it is called Bi-linear stress-strain relation.

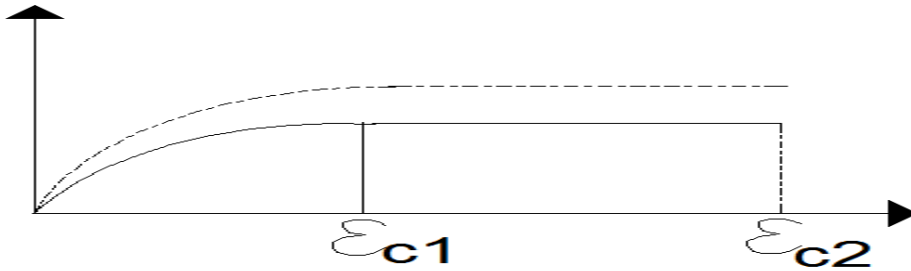


Figure 2. 23: EU 2, 1994, provision for Parabolic-rectangular stress-strain diagram for concrete under compression, [17]

For Parabolic-rectangular stress-strain distribution

Where $\varepsilon_{c1} = 2 \text{ ‰}$ and $\varepsilon_{c2} = 3.5 \text{ ‰}$

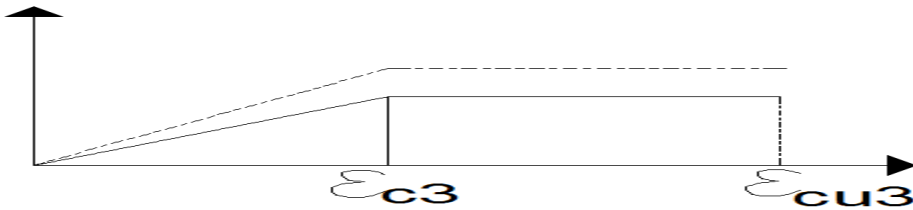


Figure 2. 24: EU 2, 1994, provision for bilinear stress-strain diagram for concrete under compression, [17]

For Bi-linear stress-strain relation.

Where $\varepsilon_{c3} = 1.75 \text{ ‰}$ and $\varepsilon_{c2} = 3.5 \text{ ‰}$

ACI 1999

The compressive strength of concrete (f_c') is determined by testing to failure 28-day-old 150mm by 300mm concrete cylinder at specified rate of loading. Although concrete are available with the 28-day ultimate strength from 15 MPa (2.5 ksi) up to 70 MPa (10 ksi) to 140 MPa (20ksi), most of the concrete used fall in to 20MPa (3ksi) to 48 MPa (7ksi).

ACI code for stress-strain curves show that the curves are roughly straight line while the load is increased from zero to one-third to one-half of the concrete ultimate strength.

Beyond this range, the behavior of the concrete becomes nonlinear. The lack of linearity of concrete stress-strain curves at higher stress causes some problems in the structural analysis.

The stress–strain curves from ACI code also shows that regardless of compressive strength, all concrete reaches their ultimate strength at strain of 0.002 ($2^0/_{00}$). From the graph it is clear that concrete does not have definite yield strength.

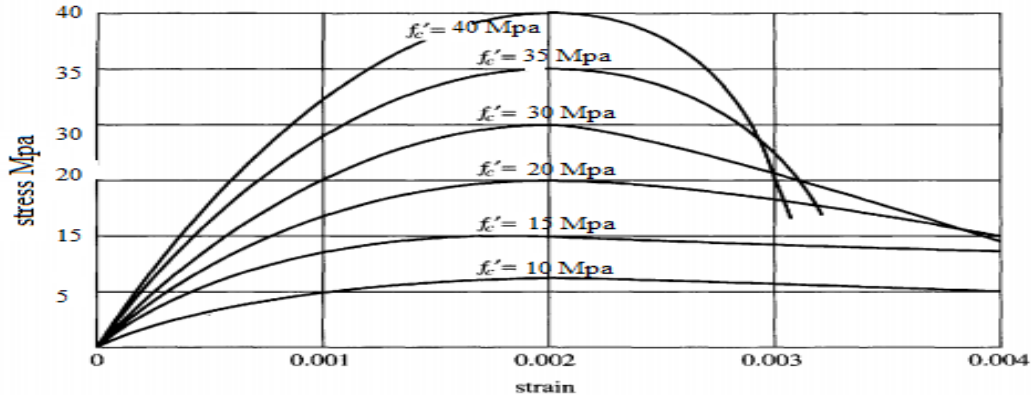


Figure 2. 25: Typical Concrete stress-strain curve according to ACI provision, [10]

2.4.3 Effect of size on the stress strain diagram

The performance of concrete was assumed to be dependent on the concrete quality. However, real life experiences shows that it is not only the concrete quality but also the size of the structure which can control the failure mechanism. The behavior and strength of reinforced concrete member is controlled by size and shape of the member and by the stress-strain properties of concrete and reinforcement.

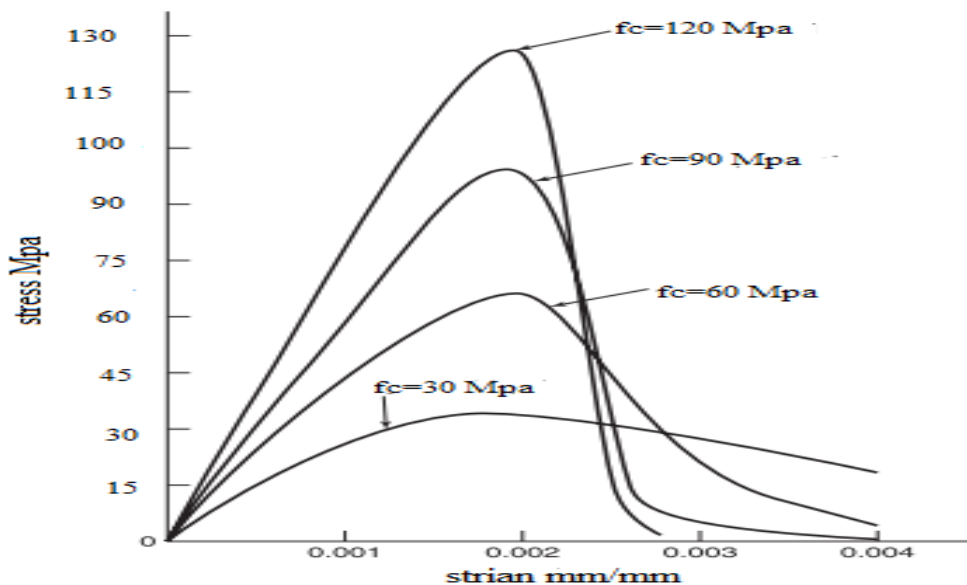


Figure 2. 26: Typical concrete stress-strain diagram under compression with different compressive strength, [10]

This stress-strain diagram has ascending and descending branches. The ascending branch is almost easy to handle due to even strain distribution. But in the descending branch there is uneven strain distribution with more or less pronounced strain localization. Therefore, the stress-strain relation should be well understood and interpreted.

Due to strain localization, stress-strain relations for post peak region shall not be used rather the stress-displacement relation can be used. For sake of analysis, it is rational to use both stress-strain relation for pre peak region and stress-displacement relation for post peak region.

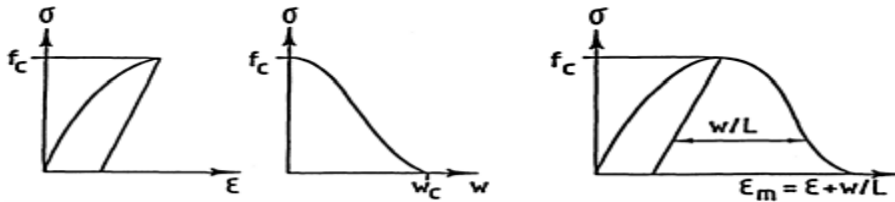


Figure 2. 27: Stress-strain and stress-displacement diagram for concrete section, [10]

The mean strain ε_m is given as:

$$\varepsilon_m = \varepsilon + \frac{w}{L}$$

Where, ε = the unloading part of the stress strain curve

L= certain length containing one localized zone

Tensile and compression failure of concrete structures can be handled by some modifications of the stress-strain curve. For normal tensile failure of concrete, the above description can fit well. But when the issue of compression failure comes in to effect, triaxial state of stress become significant and this effect has to be incorporated in to the stress-strain diagram.

In concrete structure localization can occur both on the tension and compression zone of the sections. Using the Euler beam theory which dictates that plane sections remain plane, the mean strain over the length in the stress direction can be taken as the formal concrete strain which is approximately proportional to the depth of the localized zone or the depth of the compression zone.

Based on the proportionality assumption, the ultimate strain (ε_u) can be expressed as

$$\varepsilon_u = \begin{cases} \frac{w_1}{c} & \text{Assumption I} \\ \varepsilon_0 + \frac{w_2}{c} & \text{Assumption II} \end{cases}$$

Where w_1 and w_2 are material properties while c is depth of the compression zone, [10].

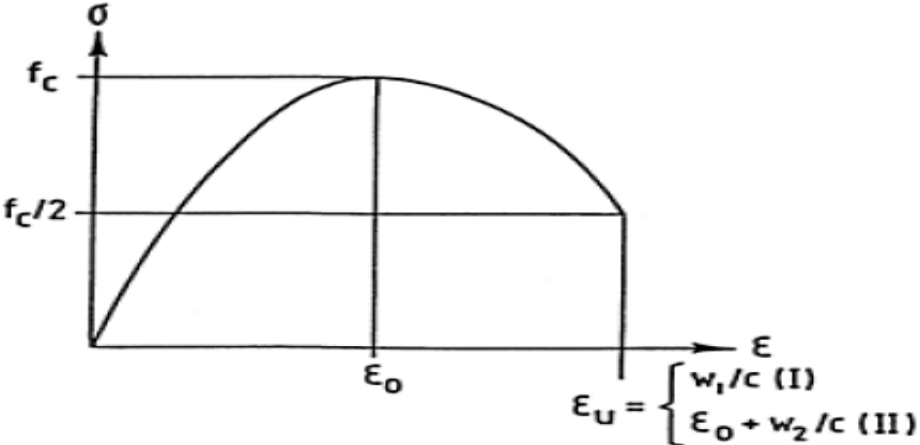


Figure 2. 28: Dependency of the stress-strain diagram in the depth of compression zone, c , [10]

3 Fracture Mechanics of Concrete

In applying Fracture Mechanics to concrete, much was initially borrowed from the wealth of information and research previously undertaken in conjunction with metals by metallurgists or mechanical engineers. However, it quickly became evident that by its very heterogeneous nature, concrete has some unique fracture characteristics, which required the alteration of existing models, [28].

By now Fracture Mechanics is universally acknowledged as a viable tool of analysis for investigation of concrete cracking. And after many years of development on numerous (plasticity based) constitutive models for concrete, tensile cracking is not yet addressed well. For the most part, even the simplest constitutive models appear to perform reasonably well under compressive regimes, however their capabilities are seriously challenged under tensile stresses. This apparent inability to properly model tensile cracking is of minor importance in reinforced concrete structures in which the steel “takes over” the tensile stresses. However, for crack related failures, the tensile strength should be properly determined for best approximation of response due to different loadings.

3.1 Pre/Post-Peak Material Response of Steel and Concrete

As an introduction to concrete Fracture, the pre- and post-peak response of Rebar’s and concrete, both obtained in a strain-controlled test of an un-cracked or un-notched specimen is shown below

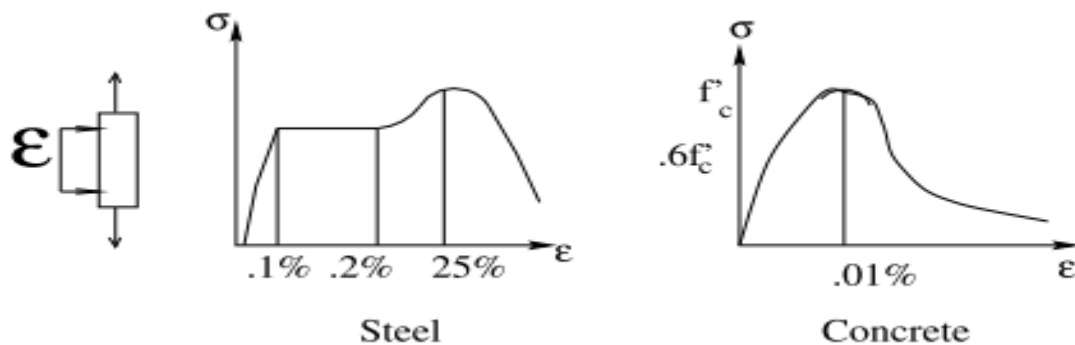


Figure 3. 1: Stress-Strain Curves of reinforcement bars and Concrete, [28]

1. Pre-peak:

(a) Reinforcement exhibits a linear elastic response up to the yield stress σ_y , and an approximate strain of 0.1%. Subsequently, due to internal dislocation and plastic deformation with strain up to 2.5% may result to be followed by strain hardening.

(b) Concrete under compression load exhibits a linear response while the load is increased from zero to about one-third to one-half of the concrete ultimate strength and with strain of approximately 0.2%. However, if the direction of the load is changed, when the load is Tensile, the concrete responds in linear manner up to approximately $0.6f'_c$ subsequently internal micro cracking induces a nonlinear response up to a peak stress f'_c and a corresponding strain of approximately 0.01%. Under load control, only the pre-peak response can be measured.

2. Post-peak:

(a) Reinforcement response in the post-peak zone is not yet well understood. Not only it is not of practical usefulness, but also it is largely overshadowed by necking.

(b) Concrete response in the post-peak zone is most interesting, as it can exhibit additional strains. The descending branch of the concrete response is an idealization of the average material response. A more accurate description should account for the localization of the induced cracks. Thus away from the localized crack there is an elastic unloading, and at the crack, since a strain cannot be properly defined, a stress-crack opening displacement is a more appropriate model.

3.2 Stress versus crack opening displacement Diagram

It is clear that concrete softening is characterized by a stress-crack opening width curve (and not stress-strain). The exact characterization of the softening response should ideally be obtained from a uniaxial test of an un-cracked specimen. However, it has been found that not only those tests are extremely sensitive, but drastically different results can be obtained from different geometries, sizes, and testing machines. Hence, the softening curve is often indirectly determined by testing notched specimens.

3.3 Concrete Models for Fracture Analysis

3.3.1 Fictitious crack model (Cohesive Crack Model)

The most referenced work in the nonlinear fracture of concrete literature, is Hillerborg Simple and elegant model which has been used for long time till the initiation the Fracture concepts. Both the experimental and theoretical Fracture concepts have been used to predict the nature of concrete near to failure stage. As mentioned in the above one of the most well-known model is the Fictitious crack model (FCM) developed by Hillerborg and co-workers. `

According to the FCM, any point on the material is in one of the three possible cases

Case 1: Undisturbed elastic state,

A point in this region is in elastic state and condition of compatibility satisfied.

Case 2: Fracture state (Fracture Zone),

The material in this region is softened by micro-cracking (Fictitious Cracks) but stress can transfer.

Case 3: No stress transformation state,

The material in this region lacks stress transfer and these are traction free surface.

All points outside the fracture zone can be handled by using the linear elastic theory. However, the points in the fracture zone is handled by special constitutive relation, the so-called stress-crack opening displacement relation, $(\sigma - w)$.

Since the traction free surface is with known boundary condition that is $\sigma_{\theta\theta} = \tau_{r\theta} = 0$ and the fracture zone is with $\sigma - w$ relation, it is rational to neglect the undisturbed elastic zone in modeling. Therefore in this model, the crack is composed of two parts, these are

1. True or physical crack across which no stresses can be transmitted. Along this zone, there is both displacement and stress discontinuities.
2. Fictitious crack, or Fracture Process Zone (FPZ) ahead of the previous one, characterized by:
 - a) Peak stress at its tip equal to the tensile strength of concrete

b) Decreasing stress distribution from f_t at the tip of the fictitious crack to zero at the tip of the physical crack. It should be noted that along the FPZ, there is displacement discontinuity and stress continuity, [28].

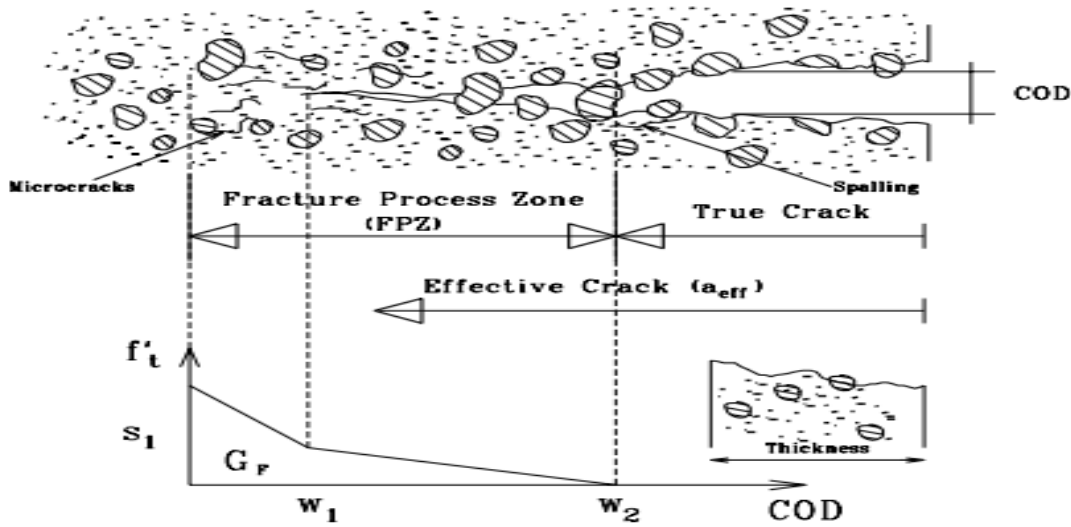


Figure 3. 2: Hillerborg Fictitious Crack Model, [28]

3.3.2 Crack Band Model (CBM)

The crack band model has been the most widely used in practice for analyzing the distributed cracking and fracture of concrete. Its main advantage over the FCM is it takes in to account tri-axial stress in the Fracture process zone (FPZ), particularly the normal and shear stress acting in the directions normal to crack plane.

The basic idea of CBM which was proposed by Bazant (1976)

- ❖ Characterize material behavior in the FPZ in Smeared manner through strain softening constitute relation
- ❖ Impose fixed width of, w_c , of the strain softening zone (crack band) representing material properties.

The imposition of constant opening width, w_c , is required in order to avoid spurious mesh sensitivity and achieve objectivity, assuring that the energy dissipation due to the fracture per unit length(and per width) is constant and equal to Fracture energy of the material.

Softening is caused by fracture strain (ϵ_f) which is superimposed to the elastic strain. Assuming all the cracks to be parallel and smeared (continuously distributed) and choosing y to be normal to the cracks (x - y plane)

$$\begin{bmatrix} \epsilon_{xx} \\ \epsilon_{yy} \\ \epsilon_{xy} \end{bmatrix} = \begin{bmatrix} c_{xxxx} & c_{xxyy} & 0 \\ c_{xxyy} & c_{yyyy} & 0 \\ 0 & 0 & \frac{c_{xyxy}}{\beta} \end{bmatrix} \begin{bmatrix} \sigma_{xx} \\ \sigma_{yy} \\ \sigma_{xy} \end{bmatrix} + \begin{bmatrix} 0 \\ 0 \\ 0 \end{bmatrix}$$

Where C matrix is the compliance matrix

$$\beta \rightarrow \rightarrow \rightarrow 0 < \beta \leq 1 \quad \text{Shear retention factor}$$

For isotropic material

$$c_{xxxx} = c_{yyyy} = \frac{1}{E'} \quad c_{yyxx} = c_{xxyy} = \frac{\nu'}{E'} \quad \text{and} \quad c_{xyxy} = \frac{2\nu'}{E'}$$

$$\text{Where, } \begin{pmatrix} E' \\ \nu' \end{pmatrix} = \begin{pmatrix} E \\ \nu \end{pmatrix} \text{ For plane stress condition} \quad \text{and} \quad \begin{pmatrix} E' \\ \nu' \end{pmatrix} = \begin{pmatrix} \frac{E}{1-\nu} \\ \frac{\nu}{1-\nu} \end{pmatrix} \text{ For plane strain condition}$$

Damage (w) is function of the strain normal to the crack, ϵ_{yy} . For no damage scenario, $w = 0$ and for complete collapse damage, $w = 1$. Therefore, w is always between 0 and 1. The fracture energy is obtained as follows

$$G_F = w_c \int_0^{\infty} \sigma_{22} d\epsilon_f$$

The fracture strain, ϵ_f , can be incorporated in terms of damage (w)

$$\epsilon_f = \left[\frac{w c_{yyyy}}{1-w} \right] \sigma_{yy}$$

New function $\Phi(\epsilon_{yy})$ can be defined as

$$\Phi \epsilon_{yy} = \frac{w}{1-w}$$

The function $\Phi(\varepsilon_{yy})$ characterizes the uniaxial stress-strain softening. There are different options in assuming $\Phi(\varepsilon_{yy})$. One of the most common is

$$\Phi(\varepsilon_{yy}) = \left(\frac{E}{f_t} \right)^a e^{-a(\varepsilon_{yy} - \varepsilon_p)}$$

Where a and ε_p are empirical constants.

The width of the crack band front can be assumed to be approximately $w_c = 3d_a$. Where d_a is the size of the maximum aggregate size. For CBM only two parameters are required and these are f_t' and G_F . The effect of w_c is very small, enough to be ignored. However, the effect of w_c will be pronounced when there are tension reinforcement (parallel cracks).

4 Application of Fracture Mechanics

4.1 Numerical Approach of Fracture Mechanics

In Fracture Mechanics only some problems have closed form solutions. This makes numerical modeling to be indispensable tool in fracture analysis. These days advanced numerical techniques are applied to study special problems like those of fracture at interface, dynamics of fracture and ductile crack growth.

The stress and strain distribution in the body caused by external and internal load can be determined in different ways. Only some of the problems have only closed form solution due to the complex stress and strain distribution. In elastic problems, Westergaard and Williams used different approaches to find stress caused by plane stress and plane strain loading.

Finite difference, Finite element and Boundary Integral Equations are well known in solid mechanics. Finite elements are also known in Fracture Mechanics and with limited cases boundary integral method can be used in Fracture analysis.

Numerical analysis are very important since they are the source of Fracture Mechanics parameters. Two way of most common approach are point matching and energy method. In point matching, stress or displacement fields are used to determine stress intensity factor (SIF). However in energy method, Energy release rate is calculated and related to stress intensity factor.

Stress and displacement matching

For Mode I fracture type and at angle $\theta = 0$

$$K_I = \lim_{r \rightarrow 0} \left[\sigma_{22} \sqrt{2\pi r} \right] \quad (4.1)$$

Where, σ_{22} is the stress acting perpendicular to the crack plane

r is the distance from the crack tip.

On the crack plane $\theta = 0$, K_I can be obtained by plotting the quantity in the square brackets against from the crack tip and extrapolate to the point $r = 0$.

4.2 SIF and propagation criteria

In LEFM, analysis of cracked bodies depends on the SIF, for mode I type SIF (K_I) can be expressed as

$$K_I = \beta \sigma_{22} \sqrt{\pi a} \quad (4.2)$$

Where, a is initial crack length, σ is remote tensile stress and β is factor considering crack geometry. For the case of central crack with length of $2a$ in infinite plate where $\beta = 1$

$$K_I = \sigma \sqrt{\pi a} \quad (4.3)$$

Since the K_I describes the nature of the stress distribution at local level, better determinations of K_I will lead to more accurate determinations of the response.

Series of Hand books are available which are used for determination of SIF. Some of which are Hand Books of SIF (Sih 1973), the stress analysis of crack Hand Book (Tada, 1971) and comparing of SIF (Rook and Carting 1976).

As long as the local material is in a linear state, principle of superposition can be used. As long as the location of the crack is fixed, SIF due to different loading can be super imposed while the material is in the linear state.

Generally there are two solution techniques which are used to solve any 2D structural geometry or loading situations. The first method involves the generations of the stress for the un cracked body part along the expected path of crack propagation. In the second method, generations of SIF via integral calculation that employs the stress obtained from the un cracked body analysis. The Green functions and the weight functions techniques can be used for integral calculation

Crack propagation

Mode I failure predominates for homogenous isotropic material. For conservative Fracture based design, one needs to characterize the crack under mixed mode loading. In mixed mode type of crack propagation, K_I and K_{II} , attains material independent critical value in space and this space is called Fracture Surface. The fracture surface can be expressed as

$$f_1 K_I, K_{II}, K_{IC}, K_{IIC}, = 0 \quad (4.4)$$

The function describing the failure surface can be expressed either by using polynomial or power law and is expressed in non-dimensional form as follows

$$\left(\frac{K_I}{K_{IC}} \right)^a + \left(\frac{K_{II}}{K_{IIC}} \right)^b = 1$$

Where a and b are obtained from material type.

However, if the energy principle is used for fracture surface function, the failure surface can be expressed as follows

$$a_{11}K_I^2 + 2a_{12}K_IK_{II} + a_{22}K_{II}^2 = a$$

Where, a_{11} , a_{12} and a_{22} are material dependent constants and a is real number constant.

Experimental evidences shows that most failure surface follow ellipse like distribution where a = b = 2.

$$\left(\frac{K_I}{K_{IC}} \right)^2 + \left(\frac{K_{II}}{K_{IIC}} \right)^2 = 1$$

The most common crack propagation criteria are

❖ Modified Griffith criteria

The concept of energy balance is extended to include energy release rates associated with all mixed mode.

$$G = G_I + G_{II}$$

Crack extends when

$$\frac{\partial G_\theta}{\partial \theta} = 0 \quad \text{and} \quad \frac{\partial^2 G_\theta}{\partial^2 \theta} < 0$$

❖ Maximum Tangential stress criteria

When a cracked body is subjected to Mode I and Mode II loading, stress will develop in the vicinity of the crack tip. According to this criteria, crack develops in the direction of maximum tangential stress.

$$\begin{bmatrix} \sigma_{rr} \\ \sigma_{\theta\theta} \\ \tau_{r\theta} \end{bmatrix} = K_I \quad K_{II} \begin{bmatrix} f_{11} & f_{21} & f_{31} \\ f_{12} & f_{22} & f_{32} \end{bmatrix}$$

Where $f_{ij}(\theta) = f(r, \theta)$

Crack extends in a direction of θ where,

$$\frac{\partial \sigma_{\theta\theta}}{\partial \theta} = 0 \quad \text{and} \quad \frac{\partial^2 \sigma_{\theta\theta}}{\partial^2 \theta} < 0$$

❖ Strain energy density criteria

According to this criteria, stress will follow a direction of minimum strain energy density.

Energy density function, W

$$W = \frac{dU}{dV}$$

Where, U is total elastic energy and V is total volume.

For linear 2D elasticity problems

$$W = \frac{1+\nu}{2E} \left[\frac{k+1}{4} (\sigma_{11} + \sigma_{22})^2 - 2\sigma_{11}\sigma_{22} - \tau_{12}^2 \right]$$

$$\text{Where, } k = \begin{cases} 3-4\nu & \text{for plane strain} \\ \frac{3-\nu}{1+\nu} & \text{for plane stress} \end{cases}$$

Crack propagates in a direction of minimum strain energy density

$$\frac{dW}{d\theta} = 0 \quad \text{and} \quad \frac{d^2W}{d^2\theta} > 0$$

4.3 Proposed crack propagation model

From the first law of thermodynamics which states about conservation of energy

$$\dot{U}_e = \dot{U}_i + \dot{U}_a + \dot{U}_d + \dot{U}_k \quad [JS^{-1}]$$

For the case of static loading $\dot{U}_k = 0$

Using variable change methods $\frac{dx}{dt} = \frac{dx}{dA} \frac{dA}{dt}$

$$\frac{du_e}{dA} = \frac{du_i}{dA} + \frac{du_a}{dA} + \frac{du_d}{dA}$$

N.B: This equation is different from Griffith energy balance, since in this equation, energy lost in the plastic zone is considered.

After some simplification

$$\frac{du_e}{dA} - \frac{du_i}{dA} - \frac{du_d}{dA} = \frac{du_a}{dA}$$

For a very small incremental area, δA , which is created due to External Loading can be calculated using differential element. Then

$$\delta A = \delta(ab)$$

Where, δa is small increment in crack length and δb is small increment in thickness

$$\delta A = b \delta a + a \delta b$$

For constant thickness $\delta b = 0$, and $\delta A = dA$, $b \delta a = b da$

$$\delta A = dA = b \delta a = b da$$

After rearranging and simplifying, finally the first Law of Thermodynamics will take the following format

$$bG' = \frac{du_e}{dA} - \frac{du_i}{dA} - \frac{du_d}{dA} = \frac{du_a}{dA}$$

Where, G' is modified Griffith energy release rate which consider the energy dissipated by plastic deformation.

For the case of fixed grips where displacement is zero..... $\frac{du_e}{dA} = 0$

This implies

$$G' = -\frac{1}{b} \left[\frac{du_i}{da} + \frac{du_d}{da} \right] \quad (4.5)$$

Typical example

Given

- ❖ In through elliptic hole
- ❖ Major and minor axis are $2a$ and $2b$ respectively
- ❖ Tensile stress at far distance from the hole (flaws)

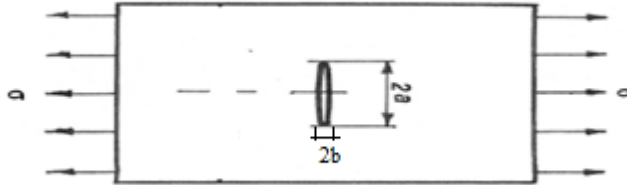


Figure 4. 1: Plate subjected to far field tensile stress with central hole,

$u_a = 4ab\gamma_s$ Surface energy dissipated to create new surface

U_i internal strain energy

$$U_i = \int_v \left(\int_0^\epsilon \sigma d\epsilon \right) dV = 2 * \left(\frac{1}{2} * 2a * \lambda a * b * \frac{\sigma^2}{2E} \right) = \frac{2a^2 \lambda b \sigma^2}{E}$$

For thin plate $\lambda = \frac{n}{2}$

$$U_i = \frac{\pi a^2 b \sigma^2}{E} \tag{4.6}$$

U_d energy dissipated by plastic deformation

$$U_d = \int_v \left(\int_0^\epsilon \sigma_{ij} - \sigma_{ij}^b d\epsilon_{ij} \right) dv \tag{4.7}$$

During collapse, strains are purely plastic and the section has two parts

The most outer part will be in plane stress mode with plastic zone of

$$r_y \theta = \frac{1}{4\pi} \left(\frac{K_I}{f_t} \right)^2 \left[1 + \cos \theta + \frac{3}{2} \cos^2 \theta \right]$$

While the most inner part will be in the plane strain mode with plastic zone of

$$r_y \theta = \frac{1}{4\pi} \left(\frac{K_I}{f_t} \right)^2 \left[(1 - 2\nu)^2 (1 + \cos \theta) + \frac{3}{2} \sin^2 \theta \right] \quad (4.8)$$

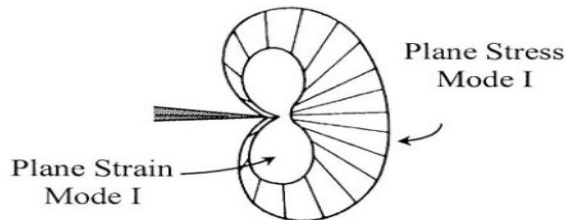


Figure 4. 2: The plane stress and plane strain plastic zone, [5]

The area of the plastic zone is assumed as the area of special curve which is shown below

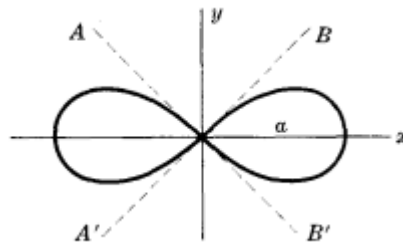


Figure 4. 3: Area of special curve called Lemniscate,

One problem with this type of special curve is the energy lost in the shaded region is not captured.

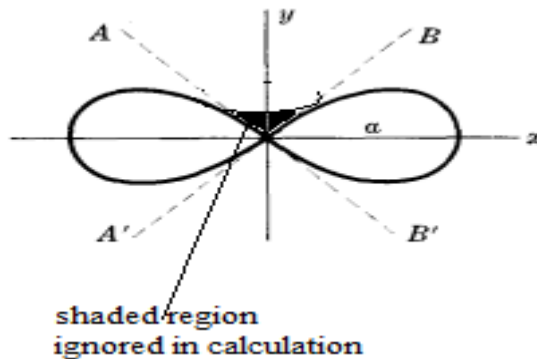


Figure 4. 4: Approximate process zone beyond crack tip

Ignoring the shaded region is conservative in the design process and it will not cause any overestimation of the maximum load to be carried by the structure.

The area of the lemniscate is about

$$A = \frac{1}{2} a^2 \quad (4.9)$$

Where, For plane stress condition $a = \frac{1}{4\pi} \left(\frac{K_I}{f_t} \right)^2$

For plane strain condition $a = \frac{1}{4\pi} \left(\frac{K_I}{f_t} \right)^2 (1 - 2\nu)^2$

For the sake of simplicity, take linear variation of the Plane stress and Plane strain area

$$V_i = \left(\frac{A_{PSS} + A_{PSN}}{2} \right) * b$$

Where, A_{PSS} = plane stress area, A_{PSN} = plane strain area, b = width of specimens and V_i is total volume plastic deformation considering the effect of poisons ratio.

Therefore, the energy dissipated by plastic deformation is

$$U_d = \frac{f_t^2}{2E} * V$$

And, finally

$$G' = -\frac{1}{b} \left[\frac{dU_i}{da} + \frac{dU_d}{da} \right] \quad (4.10)$$

This shows that the energy release will get higher value when plastic deformation is considered and the issue of plastic stress and plastic strain is avoided.

Crack Initiation Load

Design codes give prescription on how to calculate the cracking load using the cracking Moment. But the problem using the code prescription is that, crack can occur even below the expected cracking load due to Size Effect. Therefore, there should be away to consider the Size Effect in calculating the cracking load. For this reason, Fracture Mechanics concept will be used for cracking load calculation.

From the first law of thermodynamics under constant temperature, amount of energy required for a unit crack extension is

$$U_a = G_F * b * da$$

Where, U_a is surface energy

G_F = energy release rate

b = thickness of specimens

da = unit crack extensions

Given cross section

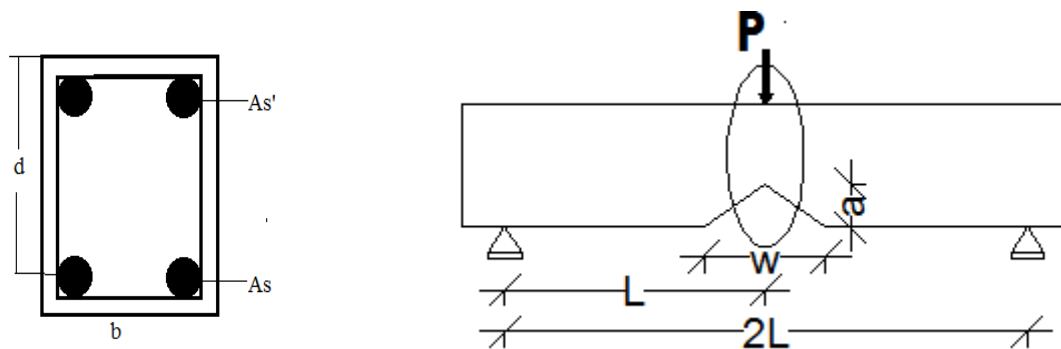
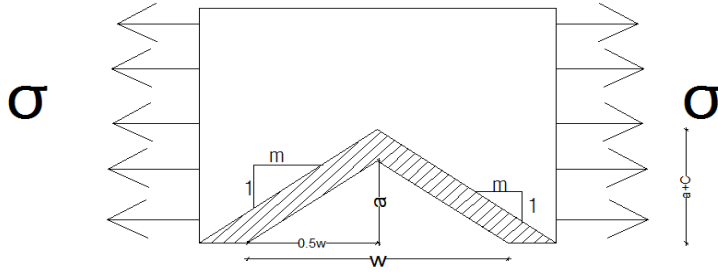


Figure 4. 5: Transverse and longitudinal section of three point bend beam

Required: The cracking Load which consider Size Effect

For the crack to nucleate, the following equilibrium condition should be satisfied



Where c is length of plastic zone, w is crack width and a is initial crack depth.

Energy dissipated by plastic deformation

$$U_d = \frac{f_t^2}{2E} * V = \frac{f_t^2}{2E} * \left(\frac{A_{PSS} + A_{PSN}}{2} \right) * b \quad (4.11)$$

Internal strain energy

$$U_i = \int_v \left(\int_0^\epsilon \sigma d\epsilon \right) dV = \frac{f_t^2}{2E} * W * c + 2mac$$

(4.12)

At the initial stage of cracking, $m = 0$ and volume of plastic zone will be

$$V = b * c * w$$

Therefore the first law of thermodynamics will take the following form

$$b * \left(\frac{f_t^2}{2E} * W * c + \frac{f_t^2}{2E} * \left(\frac{A_{PSS} + A_{PSN}}{2} \right) \right) = G'_F * \Delta a * b$$

(4.13)

After some simplification

$$\frac{f_t^3 * c * L}{8E^2} + \frac{f_t^2}{2E} \left(\frac{A_{PSS} + A_{PSN}}{2} \right) = G'_F * \frac{f_t L}{8E}$$

Rearranging the terms and after some simplification

$$f_t^2 + f_t * \frac{e}{c * L} - \frac{T}{c} = 0 \quad (4.14)$$

Where e and T are material constants obtained from Experiments.

From the above equation it is clear that tensile strength is a function of plastic zone. But it is possible to express the plastic zone size as a function of member depth as

$$c = \alpha * D$$

Therefore, Equation 4.14 can be expressed as follows

$$f_t^2 + f_t * \frac{e}{\alpha * D * L} - \frac{T}{\alpha * D} = 0 \quad (4.15)$$

Equation 4.15 shows that tensile strength of a material is a function of both member and cross section. Qualitatively Equation 4.15 shows that both depth and member length have effect on the tensile strength of the material. Therefore, Fracture is both section and member property.

Check the sensitivity of the Fracture to section and member length variation

$$\text{Let, } b_1 = \frac{e}{\alpha DL} \quad \text{and} \quad b_2 = \frac{e}{\alpha D}$$

Equation 4.15 can be reduced to the following form

$$f_t^2 + f_t * b_1 - b_2 = 0 \quad (4.16)$$

To check the sensitivity of member effect

Take D to be constant and check for

$$\frac{df_t}{dL} = 0$$

$$\text{Where } f_t^2 + f_t * \frac{e}{\alpha * D * L} - \frac{T}{\alpha * D} = 0$$

Take the derivatives and after rearranging the terms

$$\frac{df_t}{dL} = \frac{f_t * e}{2f_t \alpha DL^2 + eL}$$

To check the sensitivity cross section effect

Take L to be constant and check for

$$\frac{df_t}{dD} = 0$$

Where , $f_t^2 + f_t * \frac{e}{\alpha * D * L} - \frac{T}{\alpha * D} = 0$

Take the derivatives and after rearranging the terms

$$\frac{df_t}{dD} = \frac{f_t * e - LT}{2f_t \alpha D^2 L + eD}$$

Since $2f_t \alpha D^2 L + eD \ll 2f_t \alpha DL^2 + eL$, this shows that

$$\frac{df_t}{dD} \gg \frac{df_t}{dL}$$

The physical interpretation of the above inequality is that the tensile strength is more sensitive to the cross section than that of member length. Therefore crack nucleates whenever the applied load cause f_t amounts of tensile stress.

From the Elastic analysis for the three point bend beam

$$\sigma = \frac{6M}{bD^2} = \frac{3PL}{bD^2} \tag{4.17}$$

Where, M is the actual design moment

b is width of the cross section

D is depth of the cross section

L is half of the member length

Using Bazant size effect Law

$$\sigma_c = Bf_t \left(\frac{1}{\sqrt{1+\beta}} \right)$$

Where, B and β are parameters mainly depends on the geometry.

Equating Equation 4.17 and Bazant Size effect Law

$$\frac{3PL}{bD^2} = Bf_t \left(\frac{1}{\sqrt{1+\beta}} \right)$$

And solve for P

$$P = P_{cr} = \frac{Bf_t bD^2}{3L} \left(\frac{1}{\sqrt{1+\beta}} \right) \quad (4.18)$$

Where,

$P=P_{cr}$ is the cracking load which consider the Size Effect

f_t is tensile strength of the material

b is width of the cross section

D is depth of the cross section

L is half length of the specimen

B is empirical constant obtained from experiment data analysis

β is brittleness number obtained from experiment data analysis

Crack Propagation

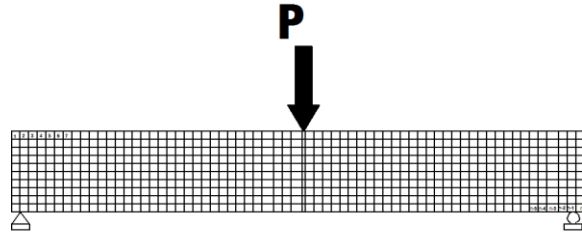


Figure 4. 6: Beam subjected to central loading

Crack follows a path where tensile strength at each element is greater than f_t and it will follow the direction of minimum tensile strength.

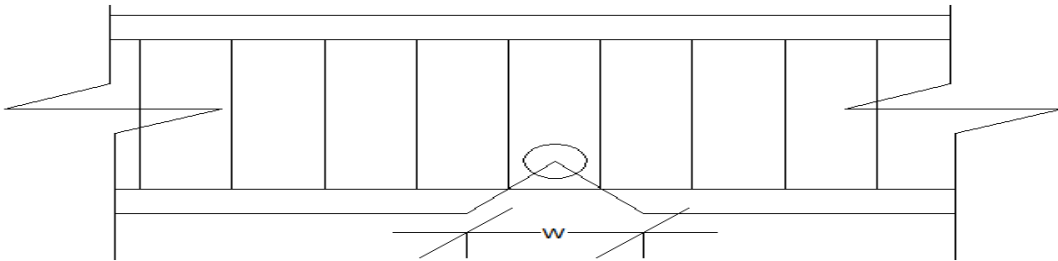


Figure 4. 7 : Beam part near the crack

At $P=P_{cr}$, crack nucleates and starts to propagate. There are two important situations occurring at this point. These are

- The existing Crack propagates
- New crack surface will start to emerges at some distance from the existing Cracks

Closure look at the crack tip

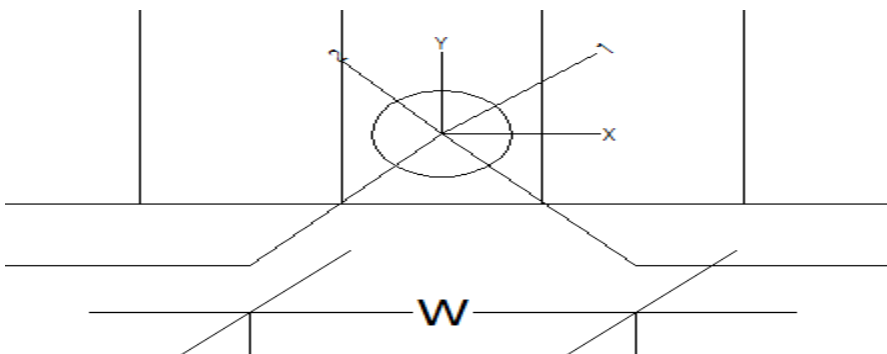


Figure 4. 8: Magnified view in the vicinity of the crack

Crack tip condition is subjected to Mode I and Mode II loading type. Take infinitesimal element at the crack tip and assume the entire shear load is carried by the concrete and neglecting the dowel action of rebar.

In the un-cracked part of the concrete

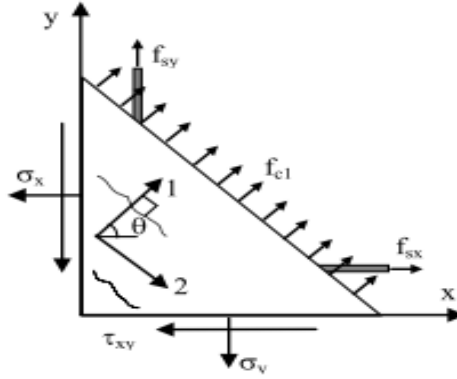


Figure 4. 9: Stress carried by rebars and concrete, [29]

Force equilibrium shows

$$\sigma_x = f_{cx} + \rho_{sx} f_{sx} \quad (4.19)$$

$$\sigma_y = f_{cy} + \rho_{sy} f_{sy} \quad (4.20)$$

Where

σ_x and σ_y are applied normal stresses in the x and y directions, respectively.

f_{cx} and f_{cy} are average concrete stresses in the x and y directions, respectively.

f_{sx} and f_{sy} are the reinforcement stresses in the x and y directions, respectively.

ρ_{sx} and ρ_{sy} are the reinforcement ratios in the x and y directions, respectively.

When the concrete section cracks, the total amount of energy entered in to the system will be dissipated by the reinforcement bars and around the crack tip by plastic deformation.

The basic assumption in the derivation of the crack propagation is that crack follows a direction of minimum resistance and to the point where the tensile strength diminishes.

Therefore, once the crack nucleates then it will follow the direction of softening tensile stress. In the post peak case, there are two sources for the tensile strength, these are tensile strength due to Tension softening and Tension Stiffening. To be on the safe side and conservatives in the design, the tensile strength due to tension softening is considered as the post cracking tensile stress.

On the way to crack propagation, some requirements should be satisfied and one of the basic parameter in cracking process is Fracture Energy. In this Thesis the fracture Energy of the concrete is taken as 75 N/M (This value is the default Value Of concrete Fracture Energy in Most Fracture Analysis Finite Element Software).

Due to simplicity and ease of application, Linear Tension Softening Model is used.



Figure 4. 10: Simple linear softening Model, [28]

From the linear Tension Softening Model

$$f_{ts} = f_{cr} \left[1 - \frac{\varepsilon_{c1} - \varepsilon_{cr}}{\varepsilon_{ch} - \varepsilon_{cr}} \right] \quad (4. 21)$$

Where, f_{ts} is Tension softened tensile strength, f_{cr} is tensile cracking stress, ε_{c1} is principal tensile stress and ε_{cr} Tensile cracking stress, ε_{ch} is characteristic strains of the tension softening Curve.

Therefore the crack follows the directions where the maximum tensile stress reaches a value of f_{ts} . The Tangential stress and shear stress in the polar coordinate

$$\sigma_{\theta\theta} = \frac{2}{\sqrt{2\pi r}} \left[K_I \left(1 + \cos \theta \cos \frac{\theta}{2} \right) + 3K_{II} \sin \theta \cos \frac{\theta}{2} \right]$$

$$\tau_{r\theta} = \frac{2}{\sqrt{2\pi r}} \left[K_I \sin \theta \cos \frac{\theta}{2} + K_{II} (3 \cos \theta - 1) \cos \frac{\theta}{2} \right]$$

Crack occurs in a direction of θ_c , where $\sigma_{\theta\theta}(\theta_c) = f_{ts}$

$$\frac{2}{\sqrt{2\pi r}} \left[K_I \left(1 + \cos \theta \cos \frac{\theta}{2} \right) + 3K_{II} \sin \theta \cos \frac{\theta}{2} \right] = f_{cr} \left[1 - \frac{\varepsilon_{c1} - \varepsilon_{cr}}{\varepsilon_{ch} - \varepsilon_{cr}} \right]$$

In addition, when the crack starts in a direction of θ_c , then $\tau_{r\theta}(\theta_c) = 0$, this means Shear stress diminishes in the crack plane. For the sake of simplicity, consider only Mode I loading in which $K_{II} = 0$.

$$\frac{2}{\sqrt{2\pi r}} \left[K_I \left(1 + \cos \theta \cos \frac{\theta}{2} \right) \right] = f_{ts}$$

For crack to Propagate, $K_I = K_{IC}$, solving for θ_c

$$\cos \theta_c = 1 - \sqrt[3]{\frac{2f_{ts}\pi r}{K_{IC}}}$$

Therefore, as long as K_{IC} , r and f_{ts} are known then the direction of the propagation can be calculated.

4.4 Proposed section capacity model

Assumption

- ✓ Water lost by evaporation from concrete structures cause additional flaws (internal micro cracks)
- ✓ Most of the fracture energy is lost in the post peak region
- ✓ Some portion of the compression zone will not carry any compressive stress due to localization

Basic points

For concrete under compression due to axial load, the ultimate strain is restricted to 0.002. However, this value is obtained from uniaxial compressive test results which needs modifications when there is general states of stress and confinements effects comes in to effect. When the loading condition is Flexure type, the ultimate strain can reach to a value of 0.0035.[4]

From the 150x150x150 concrete cube test with an approximate compression depth of 150mm, strain at ultimate is about 0.002.

From the strain distribution due to Flexure type Loading,

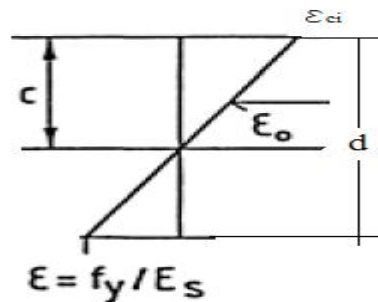


Figure 4. 11: Linear strain distribution for flexure type loading

At some concrete strain, ϵ_{ci} , is given as:

$$\frac{c_i}{d} = \frac{\epsilon_{ci}}{\epsilon_{ci} + \epsilon_s} \quad (4. 22)$$

As the total amount of energy that is going to be stored in a material and which can be used as source of energy for feature use is assumed to be constants

$$U = G_F * c * b \quad (4. 23)$$

Where U is the total energy stored, G_F is the compressive fracture energy, C is depth of compression zone and b is thickness of the material.

For constant U,

$$G_F \propto \frac{1}{c} \quad (4. 24)$$

Since the Compressive Fracture energy is directly proportional to the ultimate strain, then

$$\varepsilon_{ci} \propto \frac{1}{c} \quad (4.25)$$

This can be expressed as shown below

$$\varepsilon_{ci} = \frac{n}{c} \quad (4.26)$$

Where, n is some constant.

For initial guess of n value, take the test result from the common compressive laboratory test results where $C=150\text{mm}$ and $\varepsilon_{ci} = 0.002$. Solve for n

$$n = c * \varepsilon_{ci} = 150 * 0.002 = 0.3$$

Therefore, the strain is expressed interms of compressive zone depth

Finally

$$\varepsilon_{ci} = \frac{0.3}{c} \quad (4.27)$$

From force equilibriums

$$A_s * f_{yd} = f_{cd} * b * c \quad (4.28)$$

From strain distribution due to flexure type loading

$$\frac{c_i}{d} = \frac{\varepsilon_{ci}}{\varepsilon_{ci} + \varepsilon_s}$$

$$\frac{c_i}{d} = \frac{0.3}{\frac{0.3}{c} + \varepsilon_s}$$

$$\frac{c_i}{d} = \frac{0.3}{0.3 + c * \varepsilon_s}$$

Where, ε_s is the strain in the reinforcement and Solve for c

$$c = \frac{-0.3 + \sqrt{0.09 + 1.2 * d * \varepsilon_s}}{2\varepsilon_s} \quad (4.29)$$

The moment capacity for the given cross section is about

$$M = A_s * f_{ys} * d - 0.4 * c \quad (4.30)$$

Where, M is design moment capacity which consider the Size Effect

f_{yd} yield strength of reinforcement bars

A_s amount of reinforcement in the tension zone

d depth from most compression zone to the center of tension reinforcement bars

C depth of compression zone

4.5 Fracture Mechanics using Finite element software

Any experimental test requires lots of money, time and effort. In addition, handling of the equipment's and data recording is another critical issues. Therefore, simulations and modeling are indispensable tools for response determination of structures subjected to different loading. These simulations can be 2D or 3D. This days there are a lots of Finite Element (FE) software like those of ANSYS, NASTRAN, ADINA, COSMOS and ABAQUS which have the ability of solving very complex differential equation.

Due to the capability of predicting and displaying the pattern of crack propagation and crushing of material, and material like that of concrete can be properly represented, for this reasons FE software packages called ANSYS is selected for this study.

In ANSYS rebar's can be modeled as bar or beam elements connected to concrete mesh nodes. The concrete is modeled as SOLID 65 elements which has eight integration points. SOLID 65 elements has 3 Degree of Freedom (DOF): translation in X, Y and Z. Cracking, crushing and plastic deformation can be represented by this elements.

Fracture Analysis is a combination of stress analysis and Fracture Mechanics parameters calculation. Linear elastic or Non-linear elastic plastic methods can be used for stress analysis near

the crack tip. However, due to the high gradients of stress near the crack tips, Finite Element modeling requires special attention.

In ANSYS modeling PLANE183, 8 node quadratic element is used for 2D fracture problems and SOLID 65, 20 node brick elements is used for 3D fracture problems. In FE analysis of fracture problems, there are some important parameters which plays important role in controlling the response.

Some of the basic parameters in Fracture mechanics are

- ❖ Stress Intensity Factor(SIF)
- ❖ J integral
- ❖ C* integral
- ❖ T-stress
- ❖ Material force

From the above Fracture mechanics parameters, SIF is selected due to its ability to express the other parameters once it is accurately determined. In order for accurate calculation of SIF, there are two methods at hands; the interaction integral method and displacement extrapolation methods.

4.6 Numerical Examples

Example 1:

Given Beam cross sections

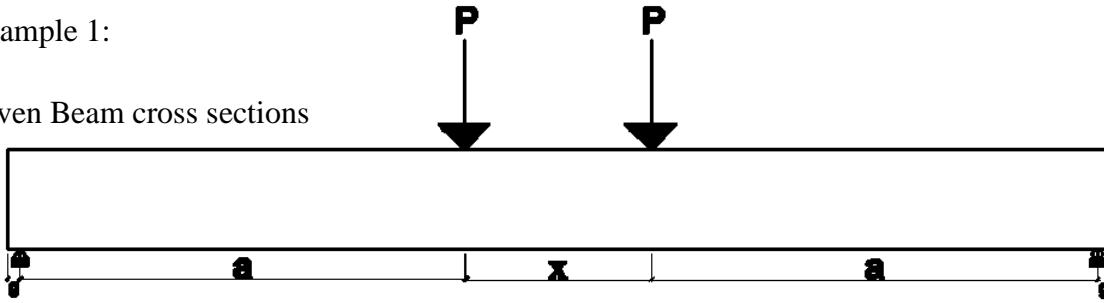
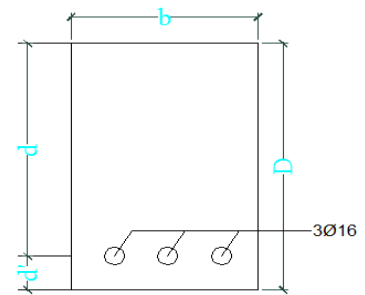


Figure 4. 12: Beam subjected to two point Loading

Dimensional information (all in mm)

Table 4. 1: Geometric parameters of the test specimens

case	D	b	a	x	L	g
1	300	200	1800	750	4235	50
2	400	200	1800	750	4235	50
3	500	200	1800	750	4235	50
4	600	200	1800	750	4235	50



Reinforcement

Table 4. 2 : Reinforcement Design Data

Beam	Bars	Asb(mm ²)	stirrups
AA	Ø 16	600mm ²	-----

For all cases, C-25 concrete is used.

Stress and strain diagram for the reinforcement

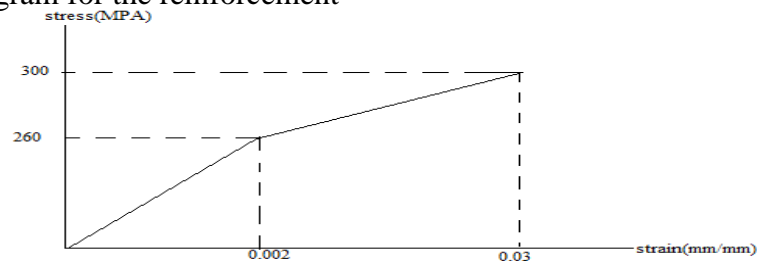


Figure 4. 13: Stress-strain diagram for reinforcement

Required

1. Calculate Cracking Load using EBCS 2, EU 2, ACI and Proposed Model
2. Calculate the maximum moments to be carried using EBCS 2, EU 2, ACI and Proposed Model
3. Use ANSYS to simulate the response

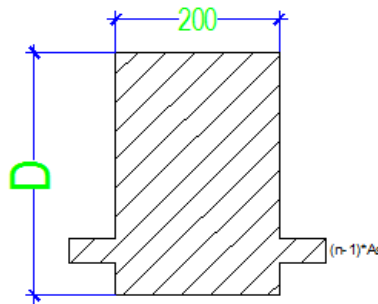
Solutions

1. Using EBCS 2

For C-25

$$f_{ck}=20 \text{ MPa} \quad f_{cd}=11.33 \text{ MPa}$$

Just before cracking, the transformed section



Where n is modular ratio expressed as shown below

$$n = \frac{E_s}{E_c} = \frac{200 \text{ GPa}}{25 \text{ GPa}} = 8$$

The gross moment of inertia, the effective neutral axis depth from the most tensile zone:

$$y = \frac{300 * 200 * 150 + 4200 * 38}{300 * 200 + 4200} = 142.67 \text{ mm}$$

$$I_g = \frac{bh^3}{12} + \sum Ad^2 = \frac{200 * 300^3}{12} + 300 * 200 * (150 - 142.67)^2 + 4200 * (142.67 - 38)^2$$

$$I_g = 4.992 * 10^8 \text{ mm}^2$$

Cracking Moments

$$M_{cr} = \frac{1.7 * f_{ctk} * I_g}{y}$$

Where $f_{ctk} = 0.21f_{ck}^{2/3} = 0.21 * 20^{2/3} = 1.5\text{MPa}$

For $f_{ctk}=1.5\text{ Mpa}$, $I_g= 4.992 * 10^8\text{mm}^2$ and $y=142.67\text{ mm}$

Therefore, the cracking moment:

$$M_{cr} = \frac{1.7 * f_{ctk} * I_g}{y}$$
$$M_{cr} = \frac{1.7 * 1.5 * 4.992 * 10^8}{142.67}$$
$$M_{cr} = 8.922\text{kN.m}$$

Since

$$M = P * a \quad \text{Solving for P}$$
$$P = \frac{M}{a} = \frac{8.922}{1.8} = 4.957\text{kN}$$

The critical Load is two times P for Four point Bend Test. Therefore, the critical Load will be

$$P_{cr} = 2 * P = 2 * 4.957 = 9.914\text{kN}$$

In the same way for the other case

Table 4. 3: EBCS 2, 1995 Critical Load

Case	D(mm)	P _{cr} (KN)
2	400	18.60
3	500	29.42
4	600	42.79

Using ACI

The Rupture Modulus

$$f_r = 0.7\sqrt{f_{ck}} = 0.7 * \sqrt{20} = 3.13\text{MPa}$$

The cracking moments will be

$$M_{cr} = \frac{f_r * I_g}{y_b} = \frac{3.13 * 4.992 * 10^8}{142.67} = 10.88 \text{ kN.m}$$

$$P_{cr} = \frac{2 * M_{cr}}{a} = \frac{2 * 10.88}{1.8} = 12.09 \text{ kN.m}$$

In the same way for the other case

Table 4. 4: ACI critical Load

Case	D(mm)	P _{cr} (KN)
2	400	22.10
3	500	35.00
4	600	50.90

Using EU 2

According to EU 2, the tensile strength is expressed as follows

$$f_{ctm} = \max \left\{ \begin{array}{l} 2.2 \\ \left(1.6 - \frac{h}{1000} \right) * f_{ctm} \end{array} \right.$$

For h = 300 mm and $f_{ctm} = 1.3 * 2.2 = 2.86 \text{ MPa}$

The cracking moments will be

$$M_{cr} = \frac{f_{ctm} * I_g}{y_b} = \frac{2.86 * 4.992 * 10^8}{142.67} = 10.007 \text{ kN.m}$$

The cracking load will be

$$P_{cr} = \frac{2 * M_{cr}}{a} = \frac{2 * 10.007}{1.8} = 11.1 \text{ kN}$$

In the same way for the other case

Table 4. 5: EC 2, 2004 Critical Load

Case	D(mm)	P _{cr} (KN)
2	400	24.24
3	500	35.19
4	600	46.50

Using the Proposed Model

The critical Load according to the proposed model is

$$P = P_{cr} = \frac{Bf_t bD^2}{3L} \left(\frac{1}{\sqrt{1+\beta}} \right) \quad \text{For three Point Bend Test with span length of } 2L.$$

Simplify the equation

$$P = P_{cr} = \frac{Bf_t bD^2}{3L} \left(\frac{1}{\sqrt{1+\beta}} \right) = \frac{bD^2}{3} * \frac{B}{L} * f_t * \left(\frac{1}{\sqrt{1+\beta}} \right)$$

$$I = \frac{bd^3}{12} = \frac{bd^2}{3} * \frac{d}{4} \quad \text{Multiply both sides by 2 where } I \text{ is the gross moment of inertia and } Y_b \text{ is}$$

the distance to most tension side from the Neutral axis.

$$2 * I = \frac{bd^3}{12} * 2 = \frac{bd^2}{3} * \frac{d}{4} * 2$$

$$\text{Solve for } \frac{bd^2}{3} \text{ and use the approximations } \frac{bd^2}{3} \simeq \frac{bD^2}{3} \text{ and } \frac{d}{2} \simeq \frac{D}{3} \simeq y_b$$

Finally use the approximations and rearrange, solve for P_{cr}

$$P_{cr} = \frac{2 * I}{y_b} * \frac{B}{a} * f_t * \left(\frac{1}{\sqrt{1+\beta}} \right)$$

Given Values

$$D=300 \text{ mm} \quad I=4.992 * 10^8 \text{ mm}^4 \quad Y_b=142.67 \text{ mm}$$

According to Koeing ,[27]

$$f_t = 2.12 \ln \left(1 + \frac{f_c}{10} \right)$$

Where f_t is tensile strength and f_c is compressive strength

For $f_c = 20 \text{ N/mm}^2$ and solve for f_t

$$f_t = 2.12 \ln \left(1 + \frac{f_c}{10} \right) = 2.12 \ln \left(1 + \frac{20}{10} \right) = 2.33 \text{ N/mm}^2$$

This tensile strength, f_t , is proposed by Koeing from experimental test results using Rumenian Shear Test where crack initiation and growth is due to other than pure tension .[27]

Assumed Value

Normally B value is obtained from experimental Data. However, the value of B obtained from statical analysis of experimental Data is itself subjected to Bias due to limited number of samples. Therefore a value B is taken to be 2 as observed from different experiments available at literatures.

The brittleness number is expressed as

$$\beta = \frac{D}{D_0} = \frac{D}{\lambda D_a} \text{ Where } D_a \text{ is the maximum aggregate size and } \lambda \text{ is some constants to be fixed}$$

from experiments. However, experts on the area recommend a value of $\lambda = 0$. use the maximum aggregate size to be 20 mm.

For the depth of $D = 300 \text{ mm}$

$$\beta = \frac{D}{D_0} = \frac{D}{\lambda D_a} = \frac{300}{3 * 20} = 5$$

Put the values in the Equation

$$P_{cr} = \frac{2I}{y_b} * \frac{B}{a} * f_t * \left(\frac{1}{\sqrt{1+\beta}} \right) = \frac{2 * 4.992 * 10^8}{142.67} * \frac{2}{1800} * 2.33 * \frac{1}{\sqrt{1+5}} = 7.39 \text{ kN}$$

Using the same procedure

Table 4. 6: Proposed Model Critical Load

b(mm)	D(mm)	Y _b (mm)	I(mm ⁴)	a=L(mm)	B	β	f _t (Mpa)	P _{cr} (KN)
200	300	142.67	499238130.8	1800	2	5	2.33	6.35
200	400	191.91	1072537022	1800	2	6.666	2.33	10.20
200	500	241.45	2091489727	1800	2	8.333	2.33	14.65
200	600	291.14	3610482935	1800	2	10	2.33	19.61

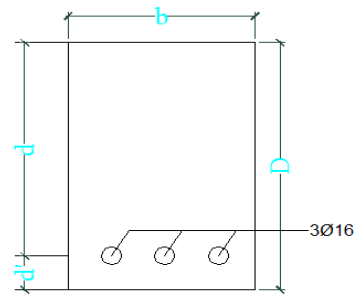
Flexural Section Capacity

ACI Design method

Nominal moment Strength calculation

For b=200mm D=300mm d'=40mm

d=D-d'=300-40=260 mm



From force equilibrium

$$T = C$$

Where T is force carried by tension rebars while C is force carried by concrete under compression. This shows that

$$A_s * f_y = 0.85f'_{ck} * b * a$$

Solving for a

$$a = \frac{A_s f_y}{0.85 * f'_{ck} * b} = \frac{600 * 300}{0.85 * 25 * 200} = 42.4 \text{ mm}$$

The nominal moment strength will be

$$M_n = T * \left(d - \frac{a}{2} \right) = A_s f_y * \left(d - \frac{a}{2} \right) = 600 * 300 * \left(260 - \frac{42.4}{2} \right) = 42.988 \text{ kN.m}$$

According to ACI design code, the strength reduction factor for flexure is about 0.9, therefore the ultimate strength of the section will be

$$M_u = 0.9 * M_n = 0.9 * 42.988 \text{ kN.m} = 38.69 \text{ kN.m}$$

Using the same principle, for the other cases

Table 4. 7: ACI moment capacity

Case	D(mm)	M _u (KN.M)
2	400	54.89
3	500	71.09
4	600	87.29

Using EU 2

According to Eurocode 2, the ultimate design moment to be carried by the given cross section is expressed as follows

$$M_{ed} = f_{cd} b d^2 \left(1 - \frac{z}{d} \right) \frac{z}{d} * 2$$

After simplifications

$$\frac{M_{ed}}{f_{cd} b d^2} = \left(1 - \frac{z}{d} \right) \frac{z}{d} * 2 = K$$

From moment equilibrium

$$M_{ed} = A_s f_{yd} * z$$

This implies that $\frac{M_{ed}}{z} = A_s f_{yd} = 600 * 260 = 156000 \text{ N}$

Using the following Equation

$$\frac{M_{ed}}{f_{cd} b d^2} * \frac{d}{2 * z} = \left(1 - \frac{z}{d} \right)$$

Solve for z, $z = 225.6 \text{ mm}$

Therefore, the moment capacity is

$$M_{ed} = A_s f_{yd} * z = 156000 * 225.6 \text{N.m}$$

$$M_{ed} = 35.194 \text{kN.m}$$

Similarly for the other cases

Table 4. 8: EU 2, 2004 Moment capacity

Case	D(mm)	M _u (KN.M)
2	400	52.55
3	500	68.11
4	600	83.11

Using EBCS 2, 1995

For concrete Grades of C-25.....Case 1

$$\text{Reinforcement ratio } \rho = \frac{A_s}{bd} = \frac{600}{200 * 260} = 0.00115$$

The ultimate moment will be

$$M_{ed} = \frac{f_{cd} b d^2}{2} \left(1 - \left(1 - \frac{\rho f_{yd}}{f_{cd}} \right)^2 \right)$$

Put $f_{cd}=11.33 \text{ MPa}$, $b=200 \text{ mm}$ $d=260 \text{ mm}$ $f_{yd}=260 \text{ MPa}$

The ultimate moment will be

$$M_{ed} = 35.09 \text{kN.m}$$

For the other cases

Table 4. 9: EBCS 2, 1995 Moment capacity

Case	D(mm)	M _u (kN.M)
2	400	50.79
3	500	66.39
4	600	81.99

Using the proposed model

The moment capacity of a given reinforced cross section is

$$M_u = A_s f_{yd} d - 0.4 * c$$

For $A_s=600 \text{ mm}^2$, $f_{yd}=260 \text{ MPa}$ and $d=260 \text{ mm}$

Calculate c, compression depth

$$c = \frac{-0.3 + \sqrt{0.09 + 1.2d\varepsilon_s}}{2\varepsilon_s}$$
$$c = \frac{-0.3 + \sqrt{0.09 + 1.2 * 260 * 0.002}}{2 * 0.002}$$
$$c = 136.25 \text{ mm}$$

Calculating the Flexural section capacity

$$M_u = A_s f_{yd} d - 0.4 * c$$
$$M_u = 600 * 260 * 260 - 0.4 * 136.25$$
$$M_u = 32.058 \text{ kN.m}$$

For the other cases

Table 4. 10: Proposed Model moment capacity

Case	D (mm)	M_u (kN.m)
2	400	45.60
3	500	59.39
4	600	73.35

Example 2:

Given: Reinforced Concrete section with depth of 300mm and width of 200mm.

$G = 75 \text{ N/M}$ $E = 30 \text{ GPa}$ $a = 50 \text{ mm}$ $f_{cr} = 2.55 \text{ Mpa}$ $\phi = 16 \text{ mm}$ $A_s = 600 \text{ mm}^2$

Req: Direction of the crack propagation using Proposed Model Crack propagation

Solution

For crack to propagate, the following criteria should be satisfied.

$$\frac{2}{\sqrt{2\pi r}} \left[K_I \left(1 + \cos \theta \cos \frac{\theta}{2} \right) \right] = f_{ts}$$

For crack to Propagate, $K_I = K_{IC}$, solving for θ_c

$$\cos \theta_c = 1 - \sqrt[3]{\frac{2f_{ts}\pi r}{K_{IC}}}$$

The critical stress intensity factor at the onset of crack propagation is, K_{IC}

$$K_{IC} = \sqrt{GE}$$

$$K_{IC} = \sqrt{75 * 30000}$$

$$K_{IC} = 1500 \text{ MPa} \sqrt{\text{mm}}$$

The post peak tensile strength is obtained from the linear tension softening model as shown below.

$$f_{ts} = f_{cr} \left[1 - \frac{\varepsilon_{c1} - \varepsilon_{cr}}{\varepsilon_{ch} - \varepsilon_{cr}} \right]$$

Where, $\varepsilon_{c1} = 0.0008$ maximum cracking strain, $\varepsilon_{c1} = 0.0008$ characteristic tensile strain

$$\varepsilon_{ch} = \frac{4G}{Sf_{cr}}$$

For cracking stress, $f_{cr} = 2.55 \text{ MPa}$, the cracking strain, ε_{cr}

$$\varepsilon_{cr} = \frac{f_{cr}}{E}$$

$$\varepsilon_{cr} = \frac{2.55}{30000}$$

$$\varepsilon_{cr} = 0.000085$$

According to EBCS 2, 1995, for humid environment, the characteristic crack width, w_k , is 0.2mm. The average distance between the cracks, S_{rm} , can be obtained from the equation shown below.

$$s_{rm} = 50 + 0.25k_1k_2 \frac{\phi}{\rho_r}$$

$k_1=0.8$, $k_2=0.5$, $\phi = 16 \text{ mm}$, $\rho_r=0.030$, put all values and obtain s_{rm}

$$s_{rm} = 50 + 0.25 * 0.8 * 0.5 * \frac{16}{0.03}$$

$$s_{rm} = 103.33\text{mm}$$

The characteristic strain, ε_{ch}

$$\varepsilon_{ch} = \frac{4G}{Sf_{cr}}$$

$$\varepsilon_{ch} = \frac{4 * 75}{0.103 * 255000}$$

$$\varepsilon_{ch} = 0.00114$$

Finally, put all values in the equation and solve for f_{ts}

$$f_{ts} = f_{cr} \left[1 - \frac{\varepsilon_{cl} - \varepsilon_{cr}}{\varepsilon_{ch} - \varepsilon_{cr}} \right]$$

$$f_{ts} = 2.55 \left[1 - \frac{0.0008 - 0.000085}{0.00114 - 0.000085} \right]$$

$$f_{ts} = 2.55\text{MPa}$$

For notched beam with pre-existing initial crack length, $a = 50\text{mm}$, and with the radius of 2mm can propagate in the direction of θ_c from the crack plane. This angle of crack propagation can be obtained from

$$\cos \theta_c = 1 - \sqrt[3]{\frac{2f_{ts}\pi R}{K_{IC}}}$$

$$\cos \theta_c = 1 - \sqrt[3]{\frac{2 * 0.8218 * 3.14 * 2}{1500}}$$

$$\cos \theta_c = 0.81$$

$$\theta = \cos^{-1} 0.81$$

$$\theta = 35.9^\circ$$

For the above condition, the crack propagates in the direction of 35.9° from the crack plane.

Example 3:

Extraction of Stress intensity Factors and Energy release rate from notched specimens

Crack length=10mm,25mm,50mm,75mm,100mm,125mm,150mm and 175 mm

Table 4. 11: initial crack length, width and length of the specimens

Crack Length a=	
Width of Beam b=	100 mm
Length of Beam L=	1000 mm

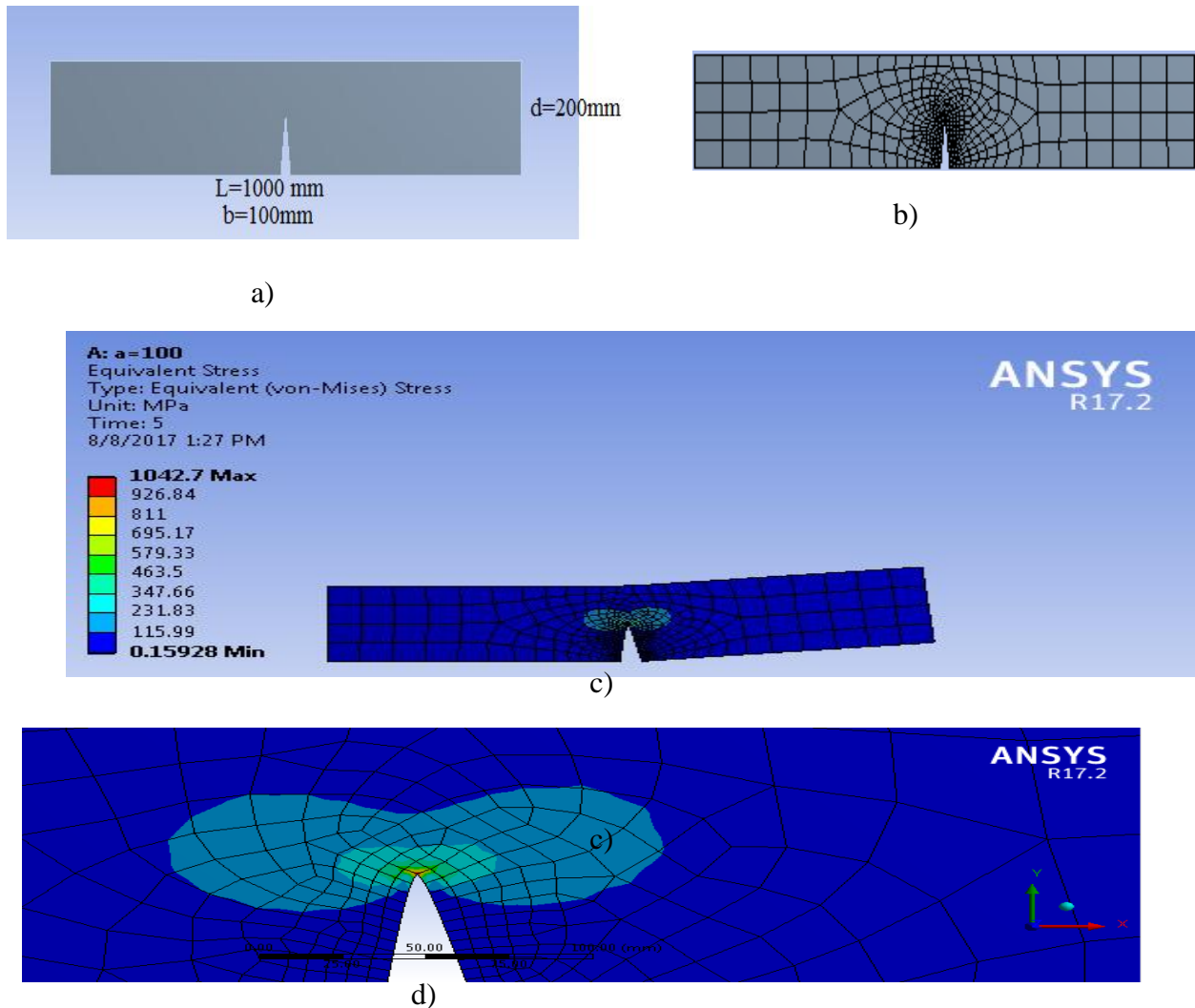


Fig: a) Notched specimen with known dimensions b) Meshing near in the vicinity of the crack

c) Stress distribution near the cracks d) Area of plastic zone near the crack

Table 4. 12: Stress intensity factors and energy release rate for plane stress and plane strain conditions

a/d	a mm	PSS			PSN		
		K_I MPa $\sqrt{\text{mm}}$	K_{II} MPa $\sqrt{\text{mm}}$	J N.mm	K_I MPa $\sqrt{\text{mm}}$	K_{II} MPa $\sqrt{\text{mm}}$	J N.mm
0.05	10	26.413	0.18577	0.023954	25.819	0.18751	0.023589
0.125	25	13.072	17.695	-6.1311E-08	13.072	17.698	2.475E-08
0.25	50	88.89	0.060035	0.27471	88.919	0.05794	0.26603
0.375	75	144.86	0.52992	0.72677	144.9	0.50838	0.7035
0.5	100	246.69	-0.27691	2.0391	246.73	-0.2768	1.9735
0.625	125	178.77	-1.2867	1.0397	179.51	-1.3145	1.015
0.75	150	209	-203.99	0.068824	208.89	-205.1	0.06805
0.875	175	636.91	-291.27	-0.23108	638.42	-294.61	-0.21803

❖ PSS refers to plane stress condition while PSN represents plane strain conditions

4.7 Comparisons and Discussions

Comparisons of Cracking Load

Table 4. 13: Cracking for different building codes under different cross section

Cracking Load in KN				
Depth	EBCS	ACI	EU	PROPOSED
300	9.91	12.09	11.12	6.35
400	18.58	21.09	24.24	10.20
500	29.42	32.41	35.19	14.65
600	42.76	46.04	46.50	19.61

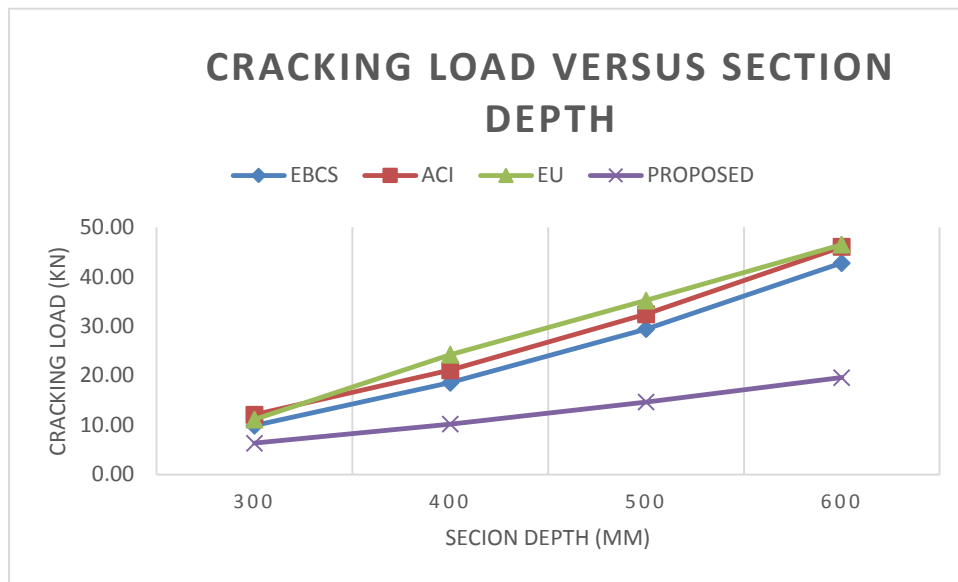


Figure 4. 14: Cracking loads versus size using different building codes and Proposed model

Discussions

From the table and the graph, it can be seen that the cracking load is proportional to the depth of the beam. As the beam depth increase, the stiffness for bending also increase. The ACI code gives relatively higher Cracking Load. One important point to be noticed here is that, almost all the building codes neglect the size effect which can be the great source of brittle failure. In the codes, the tensile strength is expressed independent of material size, this can cause an overestimation of the strength which is the main reasons why many reinforced concrete structures fail before the stress reaches to its peak value.

Comparisons of Section Moment Capacity

Table 4. 14: Moment capacity of a cross section under different building design codes and Propose model

Section Moment Capacity (KN.M)				
Depth(mm)	EBCS	ACI	EU	PROPOSED MODEL
300	35.189	38.9	35.194	30.64
400	50.79	54.89	52.5	43.68
500	66.39	71.09	68.11	57
600	81.99	87.29	83.71	70.54

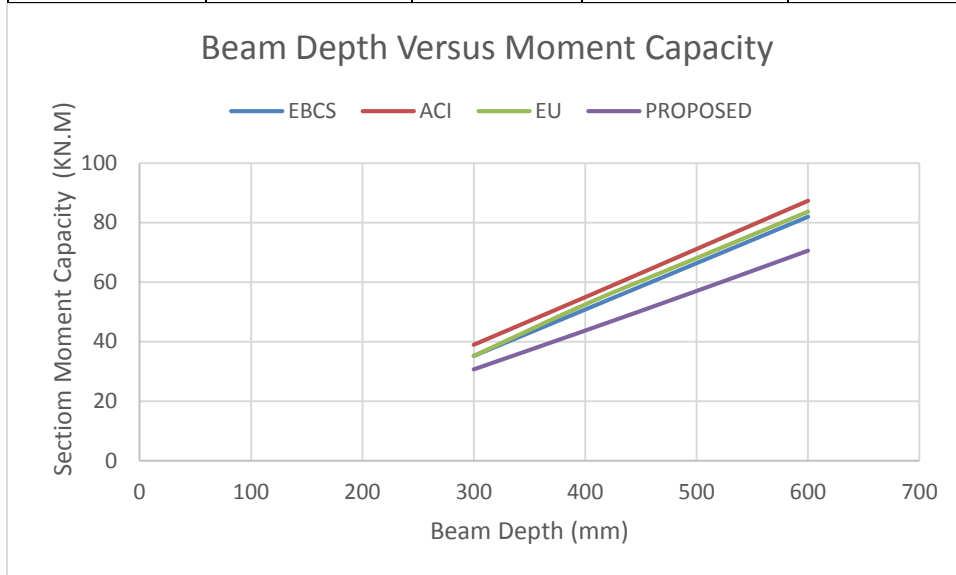


Figure 4. 15: Section capacity varies with beam size using different building codes and Proposed Model

Discussions

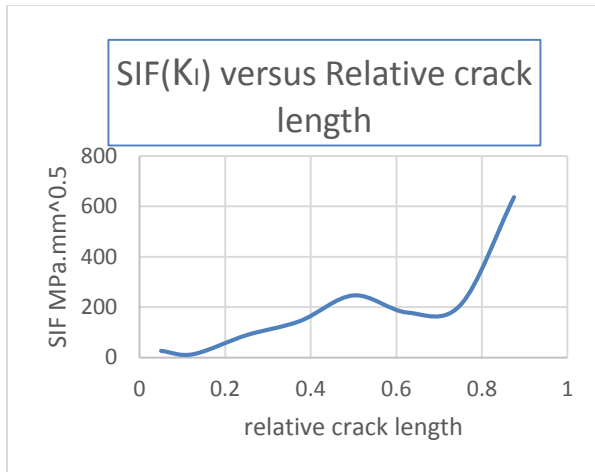
From the above data, it is clear that the moment capacity of a given beam is proportional to the depth. As in the above case, ACI code predicts the highest section moment capacity. However, the EBCS 2, 2013 and the EU 2, 2004 predicts almost the same moment capacity. But the problem with the moment capacity determined by codes is that there is no any mechanisms which consider the size effect. In the proposed model the size effect is included and the lowest section capacity is determined.

Discussion of crack propagations

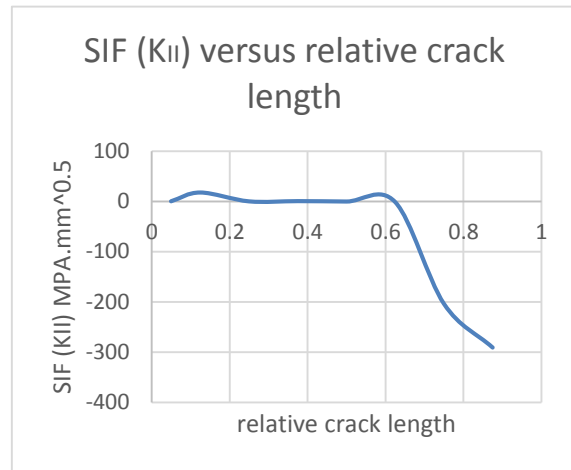
When initially notched specimen is subjected to Mode I type loading, the stress intensity factor for Mode I type of fracture will increase. The increment of the stress intensity Factor with the crack length is limited to some values of crack length. When the crack length is beyond this particular crack depth, the Mode I stress intensity factor will start to decrease and finally the specimen will collapse.

If the given specimen is subjected to Mode II type of loading, which can cause sliding, the Mode II stress intensity factor will not be effective quickly as the load is applied. However, as the effect of the Mode I stress intensity factor diminished, the Mode II stress intensity factor will become more pronounced with negative value. The negative value shows that crack occurs in the opposite direction of the loading.

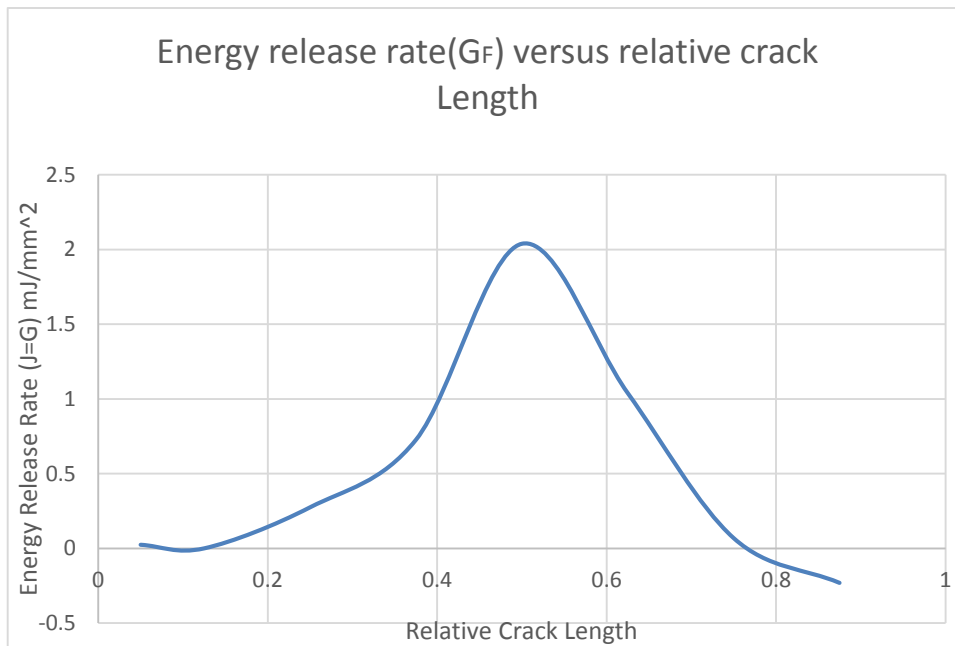
In the new proposed model, crack follows certain criteria to propagate. Once this criteria is satisfied, Crack propagates otherwise it will not. The idea of crack propagation is not yet included in many building codes. However, Using the Fracture Mechanics, it is possible to capture crack propagation.



a)



b)



c)

Figure 4. 16: a) Variations of stress intensity for mode I with proportion crack growth

b) Variations of stress intensity for mode II with crack growth c) Variations of Energy release rate for mode I and mode II with crack growth

5 Conclusion and Recommendations

5.1 Conclusions

Due to different reasons, the empirical formulas provided by Building codes do not include an important phenomena called Size Effect. This days there are huge number of construction using concrete structures in which some of them are already built and some are under constructions. As long as the need for this huge number of construction using concrete structures increases, the design principle should consider the size effect in order to have safe structure. Ignoring of size effect in this huge construction using concrete can definitely cause brittle failure which can occur at any time without any prior sign.

Real life experiences shows that as the size of the material increase, the amount of flaws and internal micro cracks also increase. What happen in the region around these flaws and micro cracks is, there will be high stress concentration, where this stress concentration around the flaws cause the development of the micro cracks in to Macro cracks. In EBCS 2, EC2 AND ACI all the empirical formulas given are independent of size which contradicts with the reality. Therefore, the effect of size on material response should be included properly to have better prediction of the response due subjected loads.

In this study, it has been also shown that Tensile Strength of reinforced concrete structure is property of member length and section. In addition the stress-strain diagram under the compressions loading is dependent on member length and section depth.

In this Thesis, there are two proposed model for Crack Propagation and Section Capacity calculation. What makes this two model differ from what has been found in the building design codes is that, the Size Effect is included in the both proposed model.

Finally, whenever the codes provisions are used, it is reasonable to assume that the codes provisions overestimate the strength, and this is mainly due to ignoring of the size effect.

5.2 Recommendations

In this thesis, it has been shown that there are some material properties, particularly tensile and compressive strength of concrete, which are assumed to be size independent. However, experiences shows that these properties are rather size dependent and some modification is mandatory when bigger section of these material is used. As long as the idea of fail-safe design is critical issues, it is better to consider the size effect on the response of a material. And from results the following recommendations are put forwarded by the Author

- ❖ Codes prescription for crack propagations and section capacity is independent of size, this will result brittle failure mode. Therefore, it is better to consider size whenever strength is critical
- ❖ Effect of size on strength and ductility of quasi brittle materials needs further study
- ❖ Structure size and geometry should be included in factor of safety to be used for reliability assessment for the design of reinforced concrete structures
- ❖ Size independent Fracture Energy should be used for Analysis and Design purpose.
- ❖ Pre-peak Fracture Energy contributions for new surface formations should be studied
- ❖ For unreinforced concrete structures which are subjected to tensile cracking, plasticity based model should be used with modification and if possible, Fracture Mechanics based model is better.

References

- [1] A.Hillerborg, M.Modeer, P.-E.Petersson: Analysis of Crack Formation and Crack Growth in Concrete by means of Fracture Mechanics and Finite Elements, Cement and Concrete Research, Vol. 6, 1976, pp 773-782.
- [2] ACI Committee 446 on Fracture Mechanics (1992) (Bazant, Z.P. prine. author & chairman).
- [3] A.R. Ingraffea. “Theory of Crack initiation and propagation in rock. In: Fracture Mechanics of Roc”. Atkinson B.K. (Ed.), Academic Press, London, pp. 71-110,1987.
- [4] American Concrete Institute Committee 318, “Building Code Requirements for Structural Concrete”, ACI 318-08, American Concrete Institute, Detroit, MI, 2008.
- [5] Anderson, D.T., Fracture Mechanics: Fundamentals and Applications. CRC Press, Boca Raton (1991)
- [6] Barenblatt, G.I. The mathematical theory of equilibrium cracks in brittle fracture. Advances in Applied Mechanics, Vol 7, 1962, pp 55-129.
- [7] Barsoum, R.S. On the use of isoparametric Finite Elements in Linear Fracture Mechanics. Int. J. Numerical Methods in Engineering, Vol 10, 1976.
- [8] Bazant ZP. Concrete Fracture Model: Testing And Practice Engineering Fracture Mechanics 69(2002)165 -205
- [9] Bazant, Z.P. and Oh. B.H. (1983) Crack band theory for fracture of concrete. RILEM, Materials and Structures, Vol 16, No 93, 155-177.
- [10] Bazant, Z.P. and Pfeiffer, P.A. (1987), “Size Effect Method for Determining Fracture Energy of Concrete from Maximum Loads of Specimens of Various Sizes”, Proposal for RILEM Recommendations.
- [11] Bazant, Z.P. (198.4), “Size Effect in Blunt Fracture: Concrete, Rock, Metals”, J. Eng. Mech., ASCE, 110, pp. 518–538.
- [12] Bazant, Z.P., 2002. “Concrete fracture models: testing and practice”. Engineering Fracture Mechanics. Vol. 69, pp. 165-205

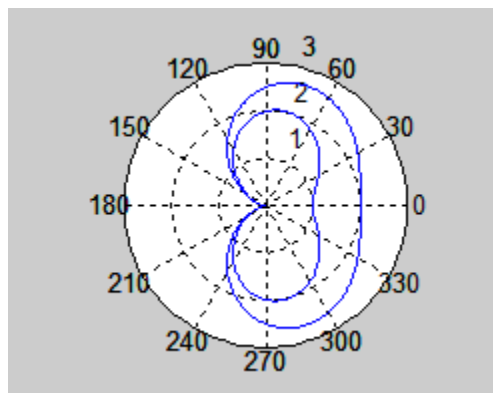
- [13] Carpinteri, A. (1984) Stability of fracturing process in RC beams. Journal of Structural Engineering (ASCE), 110,
- [14] CEB-FIP Model Code 2010, Chapter 5, Code-type models for concrete behavior (Draft); 2010.
- [15] Dr.ir. P.J.G. Schreurs. "Fracture Mechanics" Eindhoven University of Technology, Department of Engineering, Materials Technology, September 13, 2011
- [16] E. F. Rybicki and M. F. Kanninen. "Finite-element calculation of stress intensity factors by a modified crack closure integral". Engineering Fracture Mechanics, 9(4), pp. 931-938, 1977.
- [17] Eurocode 2 - Design of Concrete Structures - Part 1 (Eurocode EC 2) - prEN 1992-1-1 November 2002 [ENG].
- [18] EBCS 2,1995 - Design of Concrete Structures – Structural Use of Concrete-Addis Ababa,Ethiopia, 1995.
- [19] G.R. Irwin. "Plastic zone near a crack and fracture toughness". Proc. 7th Sagamore Conference, IV-63, New york, August 16-19, 1960.
- [20] H. Tada, P.C. Paris and G.R. Irwin. "The Stress Analysis of Cracks Handbook". Del Research Corporation, Hellertown, Pennsylvania, 1973.
- [21] H.A.W.Cornelissen, D.A.Hordijk, H.W.Reinhardt: Experiments and Theory for the Application of Fracture Mechanics to Normal and Lightweight Concrete, Contributions International Conference on Fracture Mechanics of Concrete, Lausane, 1-3 October, 1985.
- [22] Hillerborg, A. (1985), "The Theoretical Basis of a Method to Determine the Fracture Energy G_F of Concrete" Materials and Structures,
- [23]Hillerborg, A. (1988). Application of fracture mechanics to concrete: summary of a series of lectures 1988. (Report TVBM; Vol. 3030). Division of Building Materials, LTH, Lund University.
- [24] Jenq, Y.S. and Shah, S.P. (1985), "A Two Parameter Fracture Model for Concrete", J. Eng. Mech. ASCE

- [25] Karihaloo BL. Fracture Mechanics and Structural Concrete. Longman Pub Group. 1995
- [26] Koing,G.,Grimn,R. and Rimmel ,G,” shear behavior of longitudnaly reinforced concrete members of HSC”, JCI international workshop on size effect in concrete structures,pp.63-74,1993
- [27] P.A. Lagace. “Plane Stress and Plane Strain”. Lecture note Aeronautics & Astronautics and Engineering Systems, MIT, 2001.
- [28] Planas, J. and Elices, M. (1990), “A Nonlinear Analysis of a Cohesive Crack”, to be published in J. Mech. and Phys. Of Solids.
- [29] Wittman FH. Crack formation and fracture energy of normal and high strength concrete. Sadhana 2002;27(4): 413–423.
- [30] Wong,Trommels And F.J Vecchio,“ Vector2 & Formworks User’s Manual”,August 2013.

Appendix

Appendix A: Matlab code for plane strain and plane stress plastic zone

```
t = 0:.01:2*pi; nu=0.15 % % % %  
rp1=1+cos(t)+1.5*sin(t).*sin(t); % % % % PLANE STRESS PLASTIC ZONE % % % %  
rp2=(1-2*nu)^2.*(1+cos(t))+1.5*sin(t).*sin(t); % % PLANE STRAIN PLASTIC ZONE % % % %  
polar(t,rp1);  
hold on  
polar(t,rp2);
```



The internal curved Area shows the plastic plane strain zone while the outside curved zone shows zone of plastic plane stress

Appendix B: static structural simulations for two point bending

Code for concrete material

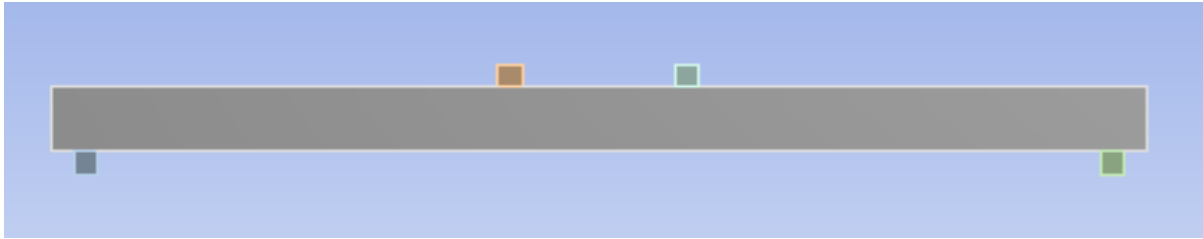
```
ET,MATID,SOLID65 ! Material definition for concrete
R,MATID,0,0,0,0,0
RMORE,0,0,0,0
MP,EX,MATID,30000 !young Modulus for concrete
MP,PRXY,MATID,0.15 ! poisson ratio for concrete
MPTEMP,MATID,22 !
TB,CONCR,MATID,1,10
TBTEMP,22
TBDATA,,0.3,0.5,2,20,0,0
TBDATA,,0,0,0.3,,
TB,MISO,MATID,1,10,0
TBTEMP,22
TBPT,,0.0001,3
TBPT,,0.0002,6
TBPT,,0.0003,9
TBPT,,0.0004,12
TBPT,,0.0015,16
TBPT,,0.0022,28
TBPT,,0.0035,20
TBPT,,0.0038,17
TBPT,,0.0042,10
TBPT,,0.0045,0
```

Code for Reinforcement material

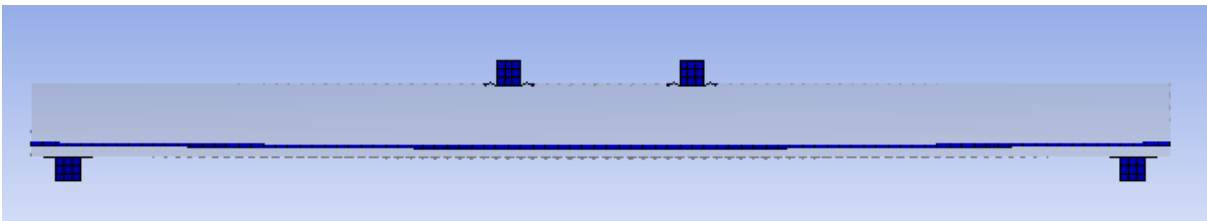
```
ET,MATID,LINK180 ! Material definition for rebars
MPDATA,EX,MATID,,2e5 ! young Modulus for rebars
MPDATA,PRXY,MATID,,0.3 !
TB,BISO,MATID,1,2
TBDATA,,280,0 !yield strength of rebars
R,MATID,8,,0!radius of rebars
```

Code for bonding between concrete and rebar (Reinforcement) elements

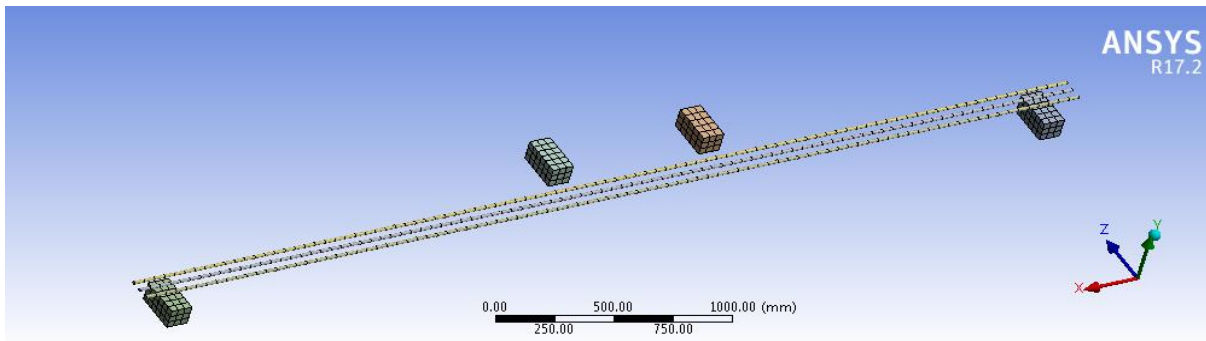
```
/PREP7
ESEL,S,ENAME,,65 !this ansys function connects all the rebars elements with the concrete
ESEL,A,ENAME,,180! Elements
ALLSEL,BELOW,ELEM !
CEINTF,0.001, !
ALLSEL,ALL !
/SOLU
OUTRES,ALL,ALL
```



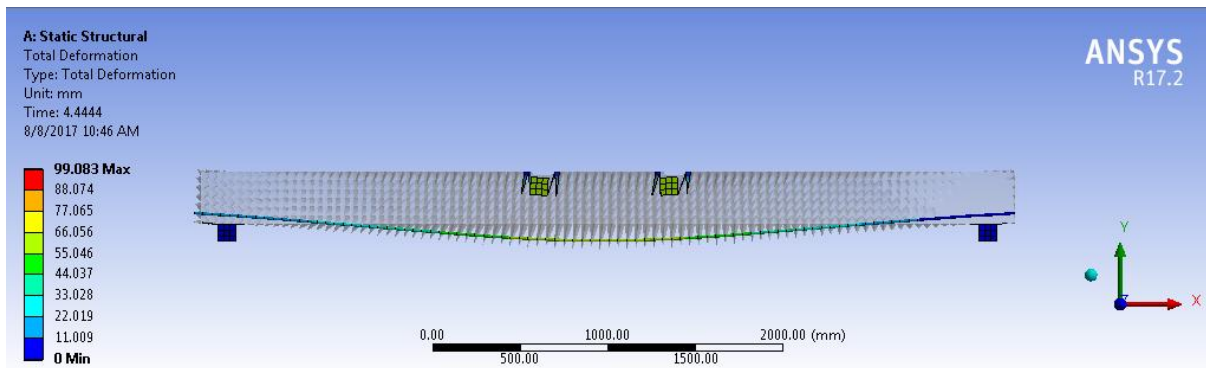
a)



b)



c)

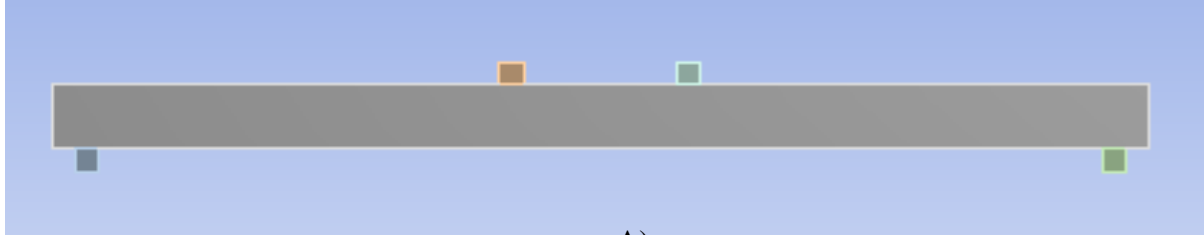


d)

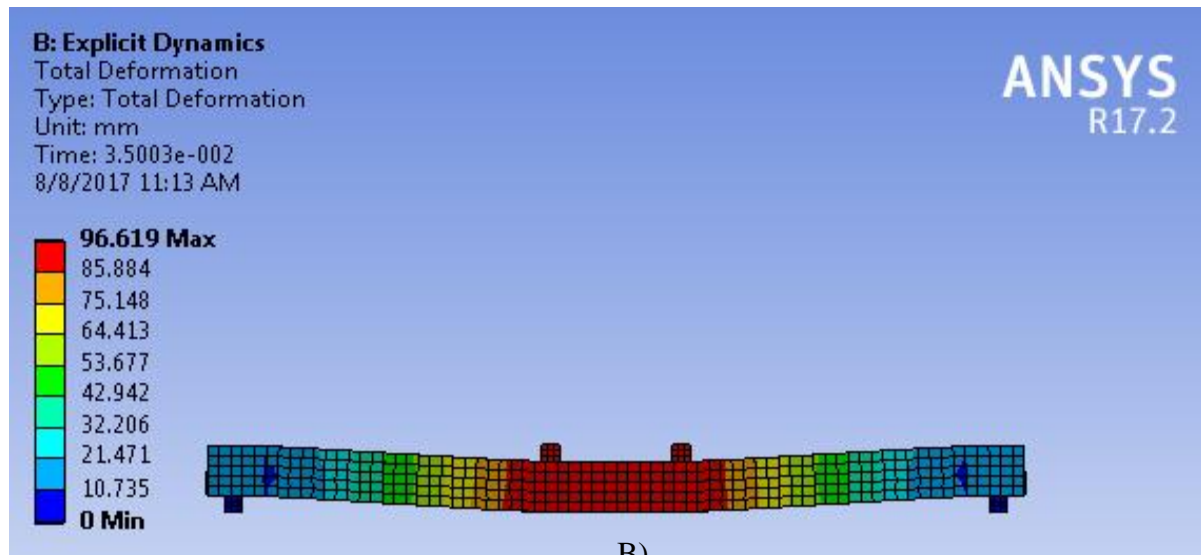
Fig a) modeling of the two point loading using ansys design model b) modeling using mechanical moduler c)impactor and rebars in the concrete d)deformed shape

Appendix C: Explicit Dynamics simulations for Four point bending

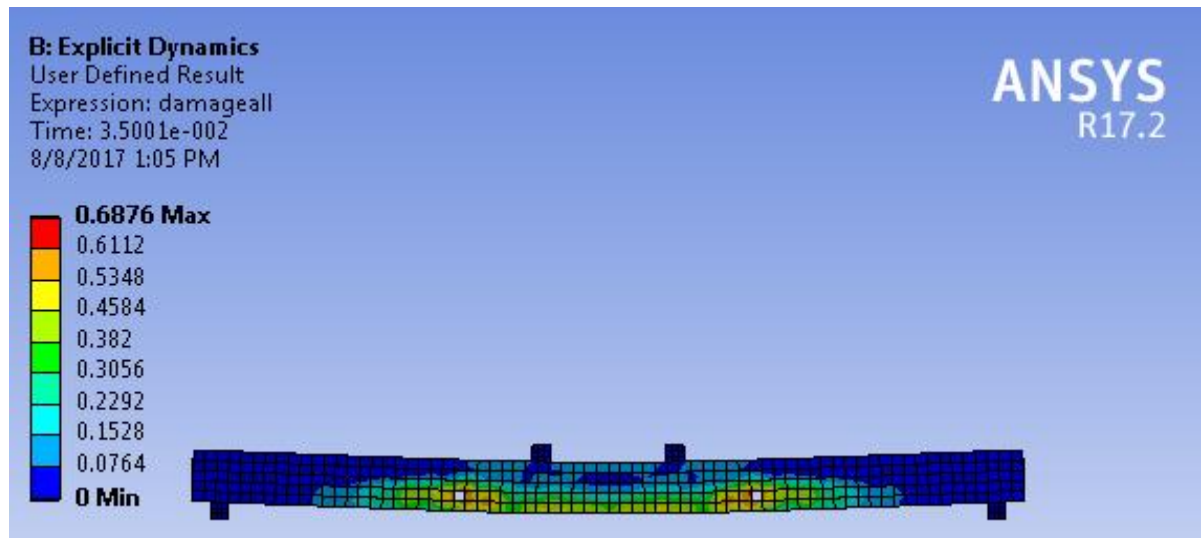
Reinforced Concrete beam with the same dimension with the static structural beam.



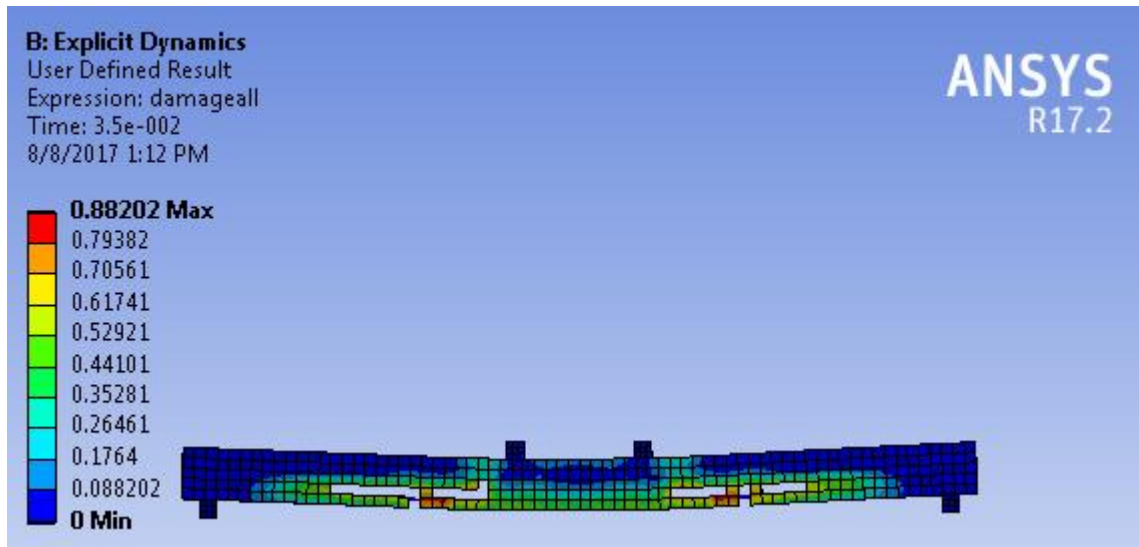
A)



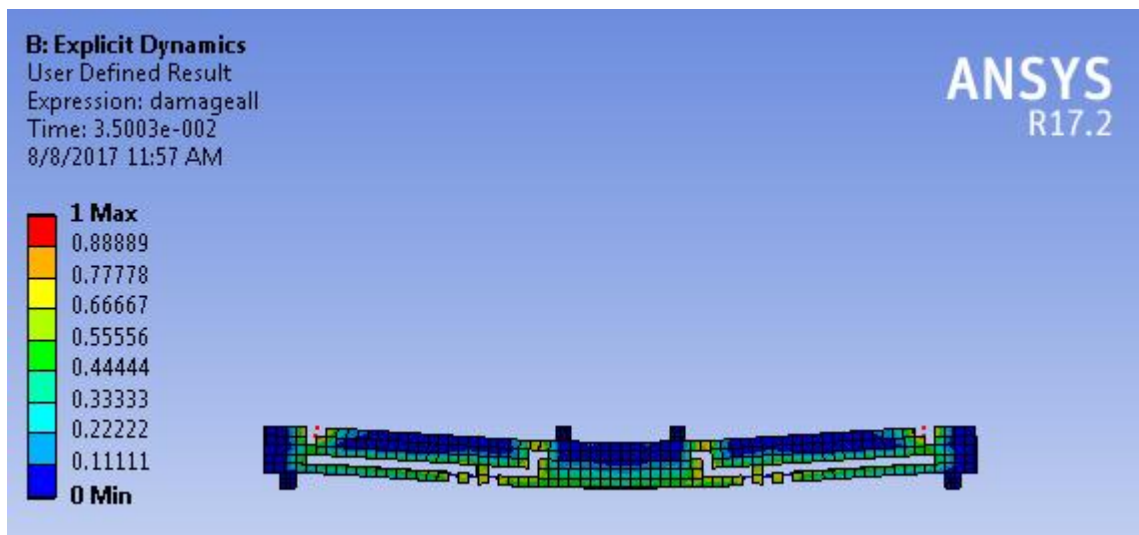
B)



C)



D)



E)

Fig R1 A) modeling for Explicit Dynamics B) Deformed shape of the beams with maximum deflections C), D) and E) shows failure steps

DECLARATION

I hereby declare that the work presented in this thesis is my original work and has not been presented for a degree in any other University and that all sources of material used for the thesis have been duly acknowledged.

Andargchew Mekonen

(Candidate)

Date

This is to certify that the above declaration made by the candidate is correct to the best of my Knowledge.

Dr.Asnake Adamu

(Thesis Advisor)

Date